Resonant contributions to three-body $B_{(s)} \to [D^{(*)}, \bar{D}^{(*)}]K^+K^-$ decays in the perturbative QCD approach

Ya Li,[1,*] Da-Cheng Yan,[2,†] Zhou Rui,[3,‡] Lan Liu,[4] Yue-Tong Zhang,[4] and Zhen-Jun Xiao[4,§]

[1]*Department of Physics, College of Sciences, Nanjing Agricultural University, Nanjing, Jiangsu 210095, People's Republic of China*

[2]*School of Mathematics and Physics, Changzhou University, Changzhou, Jiangsu 213164, People's Republic of China*

[3]*College of Sciences, North China University of Science and Technology, Tangshan 063009, People's Republic of China*

[4]*Department of Physics and Institute of Theoretical Physics, Nanjing Normal University, Nanjing, Jiangsu 210023, People's Republic of China*

(Received 31 July 2020; accepted 1 September 2020; published 17 September 2020)

In this work, we study the S, P, and D wave resonance contributions to three-body decays $B_{(s)} \to [D^{(*)}, \bar{D}^{(*)}]K^+K^-$ by employing the perturbative QCD (PQCD) approach, where the kaon-kaon invariant mass spectra are dominated by the $f_0(980)$, $f_0(1370)$, $\phi(1020)$, $\phi(1680)$, $f_2(1270)$, $f_2'(1525)$, $f_2(1750)$, and $f_2(1950)$ resonances. The KK S-wave component $f_0(980)$ is modeled with the Flatté formalism, while other resonances are described by the relativistic Breit-Wigner line shape. The corresponding decay channels are studied by constructing the kaon-kaon distribution amplitude Φ_{KK}, which captures important final state interactions between the kaon pair in the resonant region. We found that the PQCD predictions for the branching ratios for most considered decays agree with currently available data within errors. The associated polarization fractions of those vector-vector and vector-tensor decay modes are also predicted, which are expected to be tested in the near future experiments. The invariant mass spectra for the corresponding resonances in the $B_{(s)} \to [D^{(*)}, \bar{D}^{(*)}]K^+K^-$ decays are well established, which can be confronted with the precise data from the LHCb and Belle II experiments.

DOI: 10.1103/PhysRevD.102.056017

I. INTRODUCTION

Studies of nonleptonic B meson decays are crucial for testing the standard model (SM), understanding the quantum chromodynamics (QCD), and searching for the possible new physics beyond the SM. Testing the SM requires first to measure its free parameters precisely and to understand how to improve the precision of theoretical calculations. Most of the free parameters of the SM are related to flavor, such as the Cabibbo-Kobayashi-Maskawa (CKM) angles α, β, and γ. The precise measurement of the angle γ of the CKM unitarity triangle is a hot topic both in flavor physics theories and experiments. An analysis of the decays $B_{(s)} \to \bar{D}^{(*)0}\phi$ opens possibilities to offer competitive experimental precision on the angle γ [1–3]. Although the charmed decays $B_{(s)} \to D^{(*)0}\phi$ are CKM suppressed compared with the $B_{(s)} \to \bar{D}^{(*)0}\phi$ decays, they are important in the CKM angle γ extraction method. Therefore, a much deeper understanding of the related phenomena is required.

On the experimental side, more and more detailed analysis on the three-body B meson hadronic decays have been performed by the *BABAR* [4–8], Belle [9–11], and LHCb [12–19] collaborations based on the large data sample. The decay $B_s^0 \to \bar{D}^0\phi$ was first observed by the LHCb Collaboration [14]. Meanwhile, a significant signal $B^+ \to D_s^+K^+K^-$ is observed for the first time by the LHCb Collaboration [17] and a limit of $\mathcal{B}(B^+ \to D_s^+\phi) < 4.9 \times 10^{-7}(4.2 \times 10^{-7})$ is set on the branching fraction at 95% (90%) confidence level (CL). In addition, the LHCb Collaboration [18] reported their first measurement $\mathcal{B}(B_s^0 \to \bar{D}^{*0}\phi) = (3.7 \pm 0.6) \times 10^{-5}$ and gave an upper

*Corresponding author.
liyakelly@163.com
†Corresponding author.
yandac@126.com
‡Corresponding author.
jindui1127@126.com
§Corresponding author.
xiaozhenjun@njnu.edu.cn

limit $\mathcal{B}(B^0 \to \bar{D}^0\phi) < 2.3 \times 10^{-6}$ at 95% CL, where the ϕ meson is reconstructed through its decay to a K^+K^- pair.

On the theoretical side, the two-body charmed decays $B_{(s)} \to [D^{(*)}, \bar{D}^{(*)}][S, P, V, T]$ (here S, P, V, and T denote the scalar, pseudoscalar, vector, and tensor mesons) have been investigated within the framework of the PQCD factorization approach [20–26]. The channels induced by the $b \to c$ transitions are CKM favored, while those induced by the $b \to u$ transitions are CKM suppressed. Thus, the $b \to u$ decays will have smaller branching ratios. The interference between the $b \to c$ and $b \to u$ transitions gives the measurement of the CKM angle γ. As is well known, the charmed decays of $B_{(s)}$ are more complicated because of the hierarchy of the scale involved compared with the decays of $B_{(s)}$ mesons to the light vector mesons. For example, the $B \to D$ transitions involve three scales: the B meson mass m_B, the D meson mass m_D, and the mass difference from the heavy meson and the heavy quark $\bar{\Lambda} = m_B - m_b \sim m_D - m_c$, which are strikingly different from each other. Although, the factorization has been proved in soft-collinear effective theory [27], it needs more inputs than the PQCD approach. It can be found that the momentum square of the hard gluon connecting the spectator quark is only a factor of $(1 - m_D^2/m_B^2)$ to that of the $B \to$ light transitions for $B \to D$ transitions, which ensures that PQCD can also work well in $B \to D$ transitions. There are also many other traditional methods and approaches to estimate the $B \to D$ transitions, such as the heavy quark effective theory [28,29], light cone sum rules [30–32], and lattice QCD [33–35].

As addressed before, the $B \to DKK$ decay is expected to proceed through a $\phi \to KK$ intermediate state. Moreover, this process can also be dominated by a series of other resonances in S, P, and D waves. In this work, we will study the S, P, and D wave resonance contributions to three-body decays $B \to DKK$ by employing the PQCD approach, where the kaon-kaon invariant mass spectra are dominated by the $f_0(980)$, $f_0(1370)$, $\phi(1020)$, $\phi(1680)$, $f_2(1270)$, $f_2'(1525)$, $f_2(1750)$, and $f_2(1950)$ resonances. However, the theory of three-body nonleptonic decays is still in an early stage of development. Three-body B meson decay modes do receive the entangled resonant and nonresonant contributions, as well as the possible final-state interactions [36–38], whereas the relative strength of these contributions varies significantly in different regions of the Dalitz plots [39,40]. In this respect, three-body decays are considerably more challenging than two-body decays, but provide a number of theoretical and phenomenological advantages. On the one hand, the number of different three-body final states is about ten times larger than the number of two-body decays. On the other hand, each final state has a nontrivial kinematic multiplicity (a two-dimensional phase space) as opposed to two-body decays where the kinematics is fixed by the masses. This leads to a much richer phenomenology, but there is no proof of factorization for the three-body B decays at present. We can only restrict ourselves to specific kinematical configurations on the basis of the Dalitz plot analysis. The Dalitz plot contains different regions with "specifical" kinematics [41,42]. The central region corresponds to the case where all three final particles fly apart with similar large energy and none of them moves collinearly to any other. This situation contains two hard gluons and is power and α_s suppressed with respect to the amplitude at the edge. The corners correspond to the case in which one final particle is approximately at rest (i.e., soft), and the other two are fast and back-to-back. The central part of the edges corresponds to the case in which two particles move collinearly and the other particle recoils back: this is called the quasi-two-body decay. This situation exists particularly in the low $\pi\pi$ or $K\pi$ or KK invariant mass region of the Dalitz plot. Thereby, it is reasonable to assume the validity of factorization for the quasi-two-body B meson decay. Naturally the dynamics associated with the pair of final state mesons can be factorized into a two-meson distribution amplitude (DA) $\Phi_{h_1h_2}$ [43–49].

In recent years, based on the PQCD approach, more and more detailed analysis on the three-body B meson hadronic decays have been performed in the low energy resonances on $\pi\pi$, KK, $K\pi$, and $\pi\eta$ channels [50–68]. Other theoretical approaches for describing the three-body hadronic decays of B mesons based on the symmetry principles and factorization theorems have been developed. The QCD-improved factorization [69–72] has been widely adopted in the study of the three-body charmless hadronic B meson decays [42,73–84]. The U-spin and flavor $SU(3)$ symmetries were used in Refs. [85–90]. Unlike the collinear factorization in the QCD factorization approach and soft-collinear effective theory, the k_T factorization is utilized in the PQCD approach. In this approach, the transverse momentum of valence quarks in the mesons is kept to avoid the endpoint singularity [91,92]. The Sudakov factors from the k_T resummation have been included to suppress the long-distance contributions from the large-b region with b being a variable conjugate to k_T. Therefore, one can calculate the color-suppressed channels as well as the color-allowed channels in charmed B decays within the PQCD approach. The conventional noncalculable annihilation-type decays are also calculable in the PQCD approach, which is proved to be the dominant strong phase in B decays for the direct CP asymmetry.

As aforementioned for the cases of the quasi-two-body decays, the two mesons (h_1h_2) move collinearly fast, and the bachelor meson h_3 is also energetic and recoils against the meson pair in the B meson rest frame in the quasi-two-body $B \to (h_1h_2)h_3$ decays. The interaction between the meson pair and the bachelor meson is regarded as to be power suppressed. The typical PQCD factorization formula for the $B \to (h_1h_2)h_3$ decay amplitude can be described as the form of [50]

$$\mathcal{A} = \Phi_B \otimes H \otimes \Phi_{h_1h_2} \otimes \Phi_{h_3}, \tag{1}$$

where H is the hard kernel, and Φ_B and Φ_{h_3} are the universal wave functions of the B meson and the bachelor

meson, respectively. The hard kernel H describes the dynamics of the strong and electroweak interactions in three-body hadronic decays in a similar way as the one for the corresponding two-body decays. The wave functions Φ_B and Φ_{h_3} absorb the nonperturbative dynamics in the process. The $\Phi_{h_1h_2}$ is the two-hadron (KK pair in this work) DA, which involves the resonant and nonresonant interactions between the two moving collinear mesons.

The paper is organized as follows. In Sec. II, we give a brief introduction for the theoretical framework and the total decay amplitudes with the wilson coefficients and CKM matrix elements, and the amplitudes of four-quark operators needed in the calculation will be given in Sec. III. Section IV contains the numerical values and some discussions. A brief summary is given in Sec. V. The Appendix collects the explicit PQCD factorization formulas for all the decay amplitudes.

II. FRAMEWORK

A. The effective Hamiltonian and kinematics

For $B \to D^{(*)}(R \to)KK$ decays, the weak effective Hamiltonian can be specified as follows [93]:

$$\mathcal{H}_{\rm eff} = \begin{cases} \frac{G_F}{\sqrt{2}} V_{cb}^* V_{uq} [C_1(\mu)O_1(\mu) + C_2(\mu)O_2(\mu)], & \text{for } B_{(s)} \to \bar{D}^{(*)}(R \to)KK \text{ decays}, \\ \frac{G_F}{\sqrt{2}} V_{ub}^* V_{cq} [C_1(\mu)O_1(\mu) + C_2(\mu)O_2(\mu)], & \text{for } B_{(s)} \to D^{(*)}(R \to)KK \text{ decays}, \end{cases} \tag{2}$$

where $V_{cb(q)}$ and $V_{ub(q)}$ are the CKM matrix elements and R denotes the various partial wave resonances $f_0(980)$, $f_0(1370)$, $\phi(1020)$, $\phi(1680)$, $f_2(1270)$, $f_2'(1525)$, $f_2(1750)$, and $f_2(1950)$, respectively.[1] The explicit expressions of the local four-quark tree operators $O_{1,2}(\mu)$ and the corresponding Wilson coefficients $C_{1,2}(\mu)$ can be found in Ref. [93]. The q in Eq. (2) represents the quark d or s. Noted that only tree diagrams contribute to these processes, which shows that there is no direct CP asymmetry in these decays. The typical Feynman diagrams for the decays $B_{(s)} \to \bar{D}^{(*)}(R \to)KK$ and $B_{(s)} \to D^{(*)}(R \to)KK$ are shown in Figs. 1 and 2, respectively.

We will work in the B meson rest frame and employ the light-cone coordinates for momentum variables. In the light-cone coordinates, we let the kaon pair and the final-state $D^{(*)}$ move along the directions $n = (1, 0, 0_{\rm T})$ and $v = (0, 1, 0_{\rm T})$, respectively. The B meson momentum p_B, the total momentum of the kaon pair, $p = p_1 + p_2$, the final-state $D^{(*)}$ momentum p_3, and the quark momentum k_i in each meson are defined in the following form:

$$\begin{aligned} p_B &= \frac{m_B}{\sqrt{2}}(1, 1, \mathbf{0}_{\rm T}), \quad k_B = \left(0, x_B\frac{m_B}{\sqrt{2}}, \mathbf{k}_{B\rm T}\right), \\ p &= \frac{m_B}{\sqrt{2}}(1 - r_D^2, \eta, \mathbf{0}_{\rm T}), \quad k = \left(z(1 - r_D^2)\frac{m_B}{\sqrt{2}}, 0, \mathbf{k}_{\rm T}\right), \\ p_3 &= \frac{m_B}{\sqrt{2}}(r_D^2, 1 - \eta, \mathbf{0}_{\rm T}), \quad k_3 = \left(0, x_3(1 - \eta)\frac{m_B}{\sqrt{2}}, \mathbf{k}_{3\rm T}\right), \end{aligned} \tag{3}$$

where m_B is the mass of the B meson, $\eta = \frac{\omega^2}{m_B^2(1-r_D^2)}$ with $r_D = m_{D^{(*)}}/m_B$, $m_{D^{(*)}}$ is the mass of the bachelor meson, and the invariant mass squared $\omega^2 = (p_1 + p_2)^2 = p^2$. The momentum fractions x_B, z, and x_3 run from zero to unity, respectively. In the heavy quark limit, the mass difference $\bar{\Lambda}$ between b-quark (c-quark) and $B(D)$ meson is negligible.

As usual we also define the momentum p_1 and p_2 of kaon pair as

$$\begin{aligned} p_1 &= (\zeta p^+, (1 - \zeta)\eta p^+, \mathbf{p}_{1\rm T}), \\ p_2 &= ((1 - \zeta)p^+, \zeta\eta p^+, \mathbf{p}_{2\rm T}), \end{aligned} \tag{4}$$

with $\zeta = p_1^+/P^+$ characterizing the distribution of the longitudinal momentum of the kaon and $p_{1\rm T}^2 = p_{2\rm T}^2 = \zeta(1 - \zeta)\omega^2$.

B. Wave functions of B meson and the $D^{(*)}$ mesons

The light-cone matrix element of the B meson can be decomposed as [94]

$$\begin{aligned} &\int d^4z e^{i\mathbf{k}_1\cdot z}\langle 0|q_\beta(z)\bar{b}_\alpha(0)|B(p_B)\rangle \\ &= \frac{i}{\sqrt{2N_c}}\left\{(\not{p}_B + m_B)\gamma_5\left[\phi_B(\mathbf{k}_1) - \frac{\not{n} - \not{v}}{\sqrt{2}}\bar{\phi}_B(\mathbf{k}_1)\right]\right\}_{\beta\alpha}, \end{aligned} \tag{5}$$

where q represents u or d or s quark. According to the above equation, there are two different wave functions ϕ_B and $\bar{\phi}_B$ in the B meson distribution amplitudes, which obey the following normalization conditions:

$$\int \frac{d^4\mathbf{k}_1}{(2\pi)^4}\phi_B(\mathbf{k}_1) = \frac{f_B}{2\sqrt{6}}, \qquad \int \frac{d^4\mathbf{k}_1}{(2\pi)^4}\bar{\phi}_B(\mathbf{k}_1) = 0. \tag{6}$$

In general, one should consider these two Lorentz structures in the calculations of B decays as shown in

[1] In the following, we also use the abbreviation f_0, ϕ, and f_2 to denote the S, P, and D-wave resonances for simplicity.

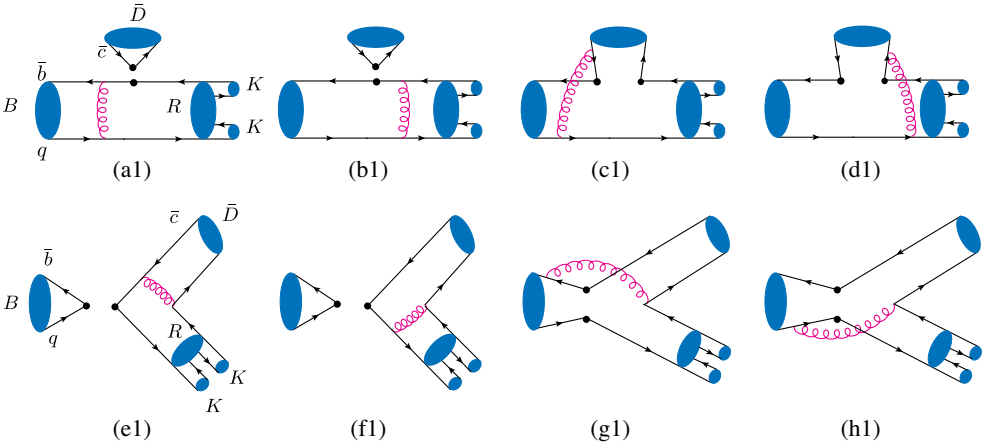

FIG. 1. Typical leading-order Feynman diagrams for the quasi-two-body decays $B \to \bar{D}^{(*)}(R \to)KK$, with $q = (u, d, s)$, and the symbol • denotes the weak vertex with the diagrams $(a1)$–$(d1)$ for the $B \to R \to KK$ transition, as well as the diagrams $(e1)$–$(h1)$ for annihilation contributions.

Ref. [95]. However, we neglect the contribution of $\bar{\phi}_B$ because of the numerical suppression in this work. Then, the wave function of the B meson can be written as [94,96–101]

$$\Phi_B = \frac{i}{\sqrt{2N_c}}(\not{p}_B + m_B)\gamma_5 \phi_B(\mathbf{k}_1), \tag{7}$$

with the widely used B-meson DA in the PQCD approach [96,98]

$$\phi_B(x,b) = N_B x^2(1-x)^2 \exp\left[-\frac{M_B^2 x^2}{2\omega_B^2} - \frac{1}{2}(\omega_B b)^2\right], \tag{8}$$

where the normalization factor N_B depends on the values of ω_B and f_B and defined through the normalization relation $\int_0^1 dx \phi_B(x, b = 0) = f_B/(2\sqrt{6})$. ω_B is a free parameter and $\omega_B = 0.40 \pm 0.04$ GeV and $\omega_{B_s} = 0.50 \pm 0.05$ GeV [96,100,101] are used in the numerical calculations. Very recently, a new method was proposed to calculate the B meson light-cone DA from lattice QCD, which can be used as an updated input for the B meson DA in the future [102].

For the $D^{(*)}$ meson, in the heavy quark limit, the two-parton light-cone DA can be written as [20–25]

$$\langle D(p_3)|q_\alpha(z)\bar{c}_\beta(0)|0\rangle = \frac{i}{\sqrt{2N_c}}\int_0^1 dx e^{ixp_3\cdot z} \times [\gamma_5(\not{p}_3 + m_D)\phi_D(x,b)]_{\alpha\beta}, \tag{9}$$

$$\langle D^*(p_3)|q_\alpha(z)\bar{c}_\beta(0)|0\rangle = -\frac{1}{\sqrt{2N_c}}\int_0^1 dx e^{ixp_3\cdot z} \times [\not{\epsilon}_L(\not{p}_3 + m_{D^*})\phi_{D^*}^L(x,b) + \not{\epsilon}_T(\not{p}_3 + m_{D^*})\phi_{D^*}^T(x,b)]_{\alpha\beta}, \tag{10}$$

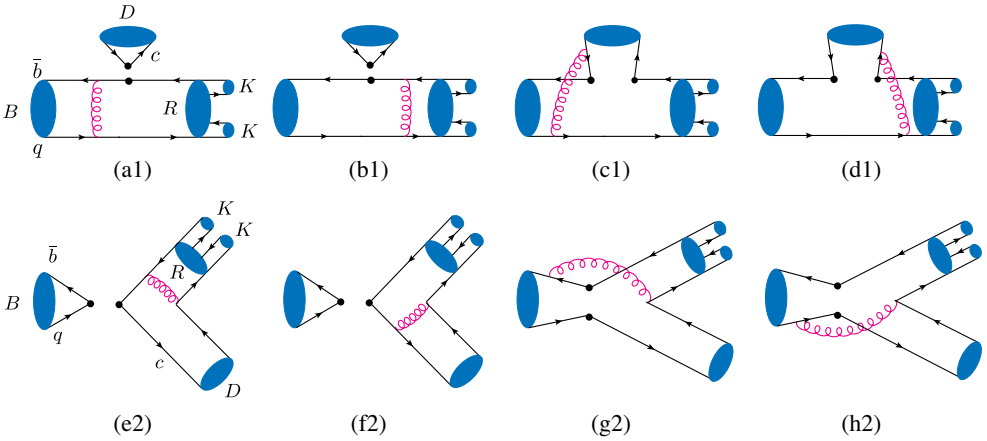

FIG. 2. Typical leading-order Feynman diagrams for the quasi-two-body decays $B \to D^{(*)}(R \to)KK$, with $q = (u, d, s)$, and the symbol • denotes the weak vertex with the diagrams $(a1)$–$(d1)$ for the $B \to R \to KK$ transition, as well as the diagrams $(e2)$–$(h2)$ for annihilation contributions.

where

$$\phi_D(x,b) = \phi_{D^*}^{L(T)}(x,b) = \frac{1}{2\sqrt{2N_c}} f_{D^{(*)}} 6x(1-x) \times [1 + C_D(1-2x)] \exp\left[\frac{-\omega^2 b^2}{2}\right], \quad (11)$$

with $C_D = 0.5 \pm 0.1, \omega = 0.1$ GeV and $f_{D^+} = 211.9$ MeV [103] for D meson. In the above models, x is the momentum fraction of the light quark in the D meson. We determine the decay constant of the vector meson D^* by using the relation $f_{D^*} = \sqrt{\frac{m_D}{m_{D^*}}} f_D$ based on the heavy quark effective theory [104].

C. Two-kaon DAs

Below, we briefly introduce the S, P, and D-wave two-kaon DAs and the corresponding timelike form factors used in our framework. It will be shown that resonant contributions through two-body channels can be included by parametrizing the two-kaon DAs. The S-wave two-kaon DAs are described in the following form [61]:

$$\Phi_S^{I=0} = \frac{1}{\sqrt{2N_c}} [\not{p}\phi_S^0(z,\zeta,\omega^2) + \omega\phi_S^s(z,\zeta,\omega^2) + \omega(\not{n}\not{p} - 1)\phi_S^t(z,\zeta,\omega^2)]. \quad (12)$$

In what follows the subscripts S, P, and D are always associated with the corresponding partial waves.

The above various twists DAs have similar forms as the corresponding twists for a scalar meson by replacing the scalar decay constant with the scalar form factor [105]. For the scalar resonances $f_0(980)$ and $f_0(1370)$, the asymptotic forms of the individual DAs in Eq. (12) have been parametrized as [43–46]

$$\phi_S^0(z,\zeta,\omega^2) = \frac{9F_S(\omega^2)}{\sqrt{2N_c}} a_S z(1-z)(1-2z), \quad (13)$$

$$\phi_S^s(z,\zeta,\omega^2) = \frac{F_S(\omega^2)}{2\sqrt{2N_c}}, \quad (14)$$

$$\phi_S^t(z,\zeta,\omega^2) = \frac{F_S(\omega^2)}{2\sqrt{2N_c}}(1-2z), \quad (15)$$

with the timelike scalar form factor $F_S(\omega^2)$ and the Gegenbauer coefficient a_S.

The P-wave two-pion DAs related to both longitudinal and transverse polarizations have been studied in Ref. [106]. Naively, the P-wave two-kaon ones can be obtained by replacing the pion vector form factors with the corresponding kaon ones. The explicit expressions of the P-wave kaon-kaon DAs associated with longitudinal (L) and transverse (T) polarization are described as follows:

$$\Phi_P^L = \frac{1}{\sqrt{2N_c}} \left[\not{p}\phi_P^0(z,\zeta,\omega^2) + \omega\phi_P^s(z,\zeta,\omega^2) + \frac{\not{n}_1\not{n}_2 - \not{n}_2\not{n}_1}{\omega(2\zeta-1)}\phi_P^t(z,\zeta,\omega^2)\right], \quad (16)$$

$$\Phi_P^T = \frac{1}{\sqrt{2N_c}} \left[\gamma_5 \not{\epsilon}_T \not{p}\phi_P^T(z,\zeta,\omega^2) + \omega\gamma_5\not{\epsilon}_T\phi_P^a(z,\zeta,\omega^2) + i\omega\frac{\epsilon^{\mu\nu\rho\sigma}\gamma_\mu\epsilon_{T\nu}p_\rho n_{-\sigma}}{p\cdot n_-}\phi_P^v(z,\zeta,\omega^2)\right]. \quad (17)$$

The two-kaon DAs for various twists are expanded in terms of the Gegenbauer polynomials:

$$\phi_P^0(z,\zeta,\omega^2) = \frac{3F_P^{\parallel}(\omega^2)}{\sqrt{2N_c}} z(1-z)\left[1 + a_{2P}^0 \frac{3}{2}(5(1-2z)^2 - 1)\right] P_1(2\zeta-1), \quad (18)$$

$$\phi_P^s(z,\zeta,\omega^2) = \frac{3F_P^{\perp}(\omega^2)}{2\sqrt{2N_c}}(1-2z)[1 + a_{2P}^s(10z^2 - 10z + 1)] P_1(2\zeta-1), \quad (19)$$

$$\phi_P^t(z,\zeta,\omega^2) = \frac{3F_P^{\perp}(\omega^2)}{2\sqrt{2N_c}}(1-2z)^2\left[1 + a_{2P}^t \frac{3}{2}(5(1-2z)^2 - 1)\right] P_1(2\zeta-1), \quad (20)$$

$$\phi_P^T(z,\zeta,\omega^2) = \frac{3F_P^{\perp}(\omega^2)}{\sqrt{2N_c}} z(1-z)\left[1 + a_{2P}^T \frac{3}{2}(5(1-2z)^2 - 1)\right]\sqrt{\zeta(1-\zeta)}, \quad (21)$$

$$\phi_P^a(z,\zeta,\omega^2) = \frac{3F_P^{\parallel}(\omega^2)}{4\sqrt{2N_c}}(1-2z)[1 + a_{2P}^a(10z^2 - 10z + 1)]\sqrt{\zeta(1-\zeta)}, \quad (22)$$

$$\phi_P^v(z,\zeta,\omega^2) = \frac{3F_P^{\parallel}(\omega^2)}{8\sqrt{2N_c}}\{[1 + (1-2z)^2] + a_{2P}^v[3(2z-1)^2 - 1]\}\sqrt{\zeta(1-\zeta)}, \quad (23)$$

with the two P-wave form factors $F_P^{\parallel}(\omega^2)$ and $F_P^{\perp}(\omega^2)$ and the Gegenbauer coefficients a_{2P}^i.

We introduce the D-wave two-kaon DAs associated with longitudinal and transverse polarizations as follows [61]:

$$\Phi_D^L = \sqrt{\frac{2}{3}}\frac{1}{\sqrt{2N_c}}\left[\not{p}\phi_D^0(z,\zeta,\omega^2) + \omega\phi_D^s(z,\zeta,\omega^2) + \frac{\not{p}_1\not{p}_2 - \not{p}_2\not{p}_1}{\omega(2\zeta-1)}\phi_D^t(z,\zeta,\omega^2)\right], \tag{24}$$

$$\Phi_D^T = \sqrt{\frac{1}{2}}\frac{1}{\sqrt{2N_c}}\left[\gamma_5\not{\epsilon}_T\not{p}\phi_D^T(z,\zeta,\omega^2) + \omega\gamma_5\not{\epsilon}_T\phi_D^a(z,\zeta,\omega^2) + i\omega\frac{\epsilon^{\mu\nu\rho\sigma}\gamma_\mu\epsilon_{T\nu}p_\rho n_{-\sigma}}{p\cdot n_-}\phi_D^v(z,\zeta,\omega^2)\right]. \tag{25}$$

The D-wave DAs are given as

$$\phi_D^0(z,\zeta,\omega^2) = \frac{6F_D^{\parallel}(\omega^2)}{2\sqrt{2N_c}}z(1-z)[3a_D^0(2z-1)]P_2(2\zeta-1), \tag{26}$$

$$\phi_D^s(z,\zeta,\omega^2) = -\frac{9F_D^{\perp}(\omega^2)}{4\sqrt{2N_c}}[a_D^0(1-6z+6z^2)]P_2(2\zeta-1), \tag{27}$$

$$\phi_D^t(z,\zeta,\omega^2) = \frac{9F_D^{\perp}(\omega^2)}{4\sqrt{2N_c}}[a_D^0(1-6z+6z^2)(2z-1)]P_2(2\zeta-1), \tag{28}$$

$$\phi_D^T(z,\zeta,\omega^2) = \frac{6F_D^{\perp}(\omega^2)}{2\sqrt{2N_c}}z(1-z)[3a_D^T(2z-1)]\mathcal{T}(\zeta), \tag{29}$$

$$\phi_D^a(z,\zeta,\omega^2) = \frac{3F_D^{\parallel}(\omega^2)}{2\sqrt{2N_c}}a_D^T(2z-1)^3\mathcal{T}(\zeta), \tag{30}$$

$$\phi_D^v(z,\zeta,\omega^2) = -\frac{3F_D^{\parallel}(\omega^2)}{2\sqrt{2N_c}}a_D^T(1-6z+6z^2)\mathcal{T}(\zeta), \tag{31}$$

with the ζ-dependent factor $P_2(2\zeta-1) = 1\text{–}6\zeta(1-\zeta)$ and $\mathcal{T}(\zeta) = (2\zeta-1)\sqrt{\zeta(1-\zeta)}$. $F_D^{\parallel,\perp}(\omega^2)$ are the D-wave timelike form factors and the Gegenbauer moments $a_D^{0,T}$ have been determined in our previous work [61].

The strong interactions between the resonance and the final-state meson pair, including elastic rescattering of the final-state meson pair, can be factorized into the timelike form factor $F_{S,P,D}(\omega^2)$, which is guaranteed by the Watson theorem [107]. For a narrow resonance, we usually use the relativistic Breit-Wigner (BW) line shape to parametrize the timelike form factor $F(\omega^2)$. The explicit expression is [108]

$$F(\omega^2) = \sum_i \frac{c_i m_i^2}{m_i^2 - \omega^2 - i m_i\Gamma_i(\omega^2)}, \tag{32}$$

where the corresponding weight coefficients c_i are determined based on the normalization condition $F(0) = 1$. The m_i and Γ_i are the pole mass and width of the corresponding resonances shown in Table I, respectively. The mass-dependent width $\Gamma_i(\omega)$ is defined as

$$\Gamma_i(\omega^2) = \Gamma_i\left(\frac{m_i}{\omega}\right)\left(\frac{|\vec{p}_1|}{|\vec{p}_0|}\right)^{(2L_R+1)}. \tag{33}$$

The $|\vec{p}_1|$ is the momentum vector of the resonance decay product measured in the resonance rest frame, while $|\vec{p}_0|$ is the value of $|\vec{p}_1|$ at $\omega = m_i$. The explicit expression of kinematic variables $|\vec{p}_1|$ is

$$|\vec{p}_1| = \frac{\sqrt{\lambda(\omega^2, m_{h_1}^2, m_{h_2}^2)}}{2\omega}, \tag{34}$$

TABLE I. Parameters used to describe intermediate states in our framework.

Resonance	Mass [MeV]	Width [MeV]	J^{PC}	Model	Source
$f_0(980)$	990	…	0^{++}	Flatté	PDG [103]
$f_0(1370)$	1475	113	0^{++}	RBW	LHCb [109]
$\phi(1020)$	1019	4.25	1^{--}	RBW	PDG [103]
$\phi(1680)$	1689	211	1^{--}	RBW	Belle [110]
$f_2(1270)$	1276	187	2^{++}	RBW	PDG [103]
$f_2'(1525)$	1525	73	2^{++}	RBW	PDG [103]
$f_2(1750)$	1737	151	2^{++}	RBW	Belle [111]
$f_2(1950)$	1980	297	2^{++}	RBW	Belle [111]

with the Källén function $\lambda(a,b,c) = a^2 + b^2 + c^2 - 2(ab + ac + bc)$. L_R is the orbital angular momentum in the dikaon system and $L_R = 0, 1, 2, \ldots$ corresponds to the $S, P, D, \ldots$ partial-wave resonances. Due to the limited studies on the form factor $F^{\perp}(\omega^2)$, we use the two decay constants $f_i^{(T)}$ of the intermediate particle to estimate the form factor ratio $r^T = F^{\perp}(\omega^2)/F^{\parallel}(\omega^2) \approx (f_i^T/f_i)$.

The BW formula does not work well for $f_0(980)$, because its pole mass is close to the $K\bar{K}$ threshold. The resulting line shape above and below the threshold of the intermediate particle is called Flatté parametrization [112]. If the coupling of a resonance to the channel opening nearby is very strong, the Flatté parametrization shows a scaling invariance and does not allow for an extraction of individual partial decay widths. If the scalar resonance lies under the $K\bar{K}$ threshold, the position of the peak in the mass spectrum does not coincide with the pole mass of the resonance. To solve the problem, the finite width to the propagator of scalar resonance has been taken into consideration by Achasov [113–115], which is the one-loop contribution to the self-energy of the scalar resonance from the two-particle intermediate states. More details can be found in Refs. [113–118]. In addition, the exponential factor $F_{KK} = e^{-\alpha q_K^2}$ with $\alpha = (2.0 \pm 0.25)$ GeV^{-2} is introduced above the $K\bar{K}$ threshold and serves to reduce the ρ_{KK} factor as the invariant mass increases, where q_K is the koan momentum in the kaon-kaon rest frame [119]. This parametrization decreases the $f_0(980)$ width above $K\bar{K}$ threshold slightly. In this work, the invariant mass of the dikaon is above the K^+K^- threshold; we have tested the impact of the self-energy correction and found it is small. Thus, we employ the modified Flatté model suggested by Bugg [119] following the LHCb Collaboration [120,121],

$$F(\omega^2) = \frac{m_{f_0(980)}^2}{m_{f_0(980)}^2 - \omega^2 - i m_{f_0(980)}(g_{\pi\pi}\rho_{\pi\pi} + g_{KK}\rho_{KK}F_{KK}^2)}. \tag{35}$$

The coupling constants $g_{\pi\pi} = 0.167$ GeV and $g_{KK} = 3.47 g_{\pi\pi}$ [120,121] describe the $f_0(980)$ decay into the final states $\pi^+\pi^-$ and K^+K^-, respectively. The phase space factors $\rho_{\pi\pi}$ and ρ_{KK} read as [112,120,122]

$$\begin{aligned}\rho_{\pi\pi} &= \frac{2}{3}\sqrt{1 - \frac{4m_{\pi^\pm}^2}{\omega^2}} + \frac{1}{3}\sqrt{1 - \frac{4m_{\pi^0}^2}{\omega^2}},\\ \rho_{KK} &= \frac{1}{2}\sqrt{1 - \frac{4m_{K^\pm}^2}{\omega^2}} + \frac{1}{2}\sqrt{1 - \frac{4m_{K^0}^2}{\omega^2}}.\end{aligned} \tag{36}$$

D. The differential branching ratio

The double differential branching ratio can be obtained as [103]

$$\frac{d^2\mathcal{B}}{d\zeta d\omega} = \frac{\tau_B \omega |\vec{p}_1||\vec{p}_3|}{32\pi^3 m_B^3}|\mathcal{A}|^2. \tag{37}$$

The three-momenta of the kaon and D meson in the KK center-of-mass frame are given by

$$|\vec{p}_1| = \frac{\sqrt{\lambda(\omega^2, m_K^2, m_K^2)}}{2\omega}, \qquad |\vec{p}_3| = \frac{\sqrt{\lambda(m_B^2, m_D^2, \omega^2)}}{2\omega}. \tag{38}$$

The complete amplitude $\mathcal{A}$ through intermediate resonances for the concerned decay channels can be written as the summation of $\mathcal{A}_S$, $\mathcal{A}_P$, and $\mathcal{A}_D$:

$$\mathcal{A} = \mathcal{A}_S + \mathcal{A}_P + \mathcal{A}_D, \tag{39}$$

where $\mathcal{A}_S$, $\mathcal{A}_P$, and $\mathcal{A}_D$ denote the corresponding three S, P, and D wave decay amplitudes.

Due to the angular momentum conservation requirement, the vector mesons $\phi, \bar{D}^*, D^*$ and tensor meson $f_2^{(\prime)}$ in the quasi-two-body decays $B_{(s)} \to (\bar{D}^*, D^*)[f_0 \to]KK$ and $B_{(s)} \to (\bar{D}, D)[\phi, f_2^{(\prime)} \to]KK$ should be completely polarized in the longitudinal direction. For $B_{(s)} \to (\bar{D}^*, D^*) \times [\phi, f_2^{(\prime)} \to]KK$ decays, both the longitudinal polarization and the transverse polarization contribute. The amplitudes can be decomposed as follows:

$$\mathcal{A}_{P(D)} = \mathcal{A}_L + \mathcal{A}_N \epsilon_T \cdot \epsilon_{3T} + i\mathcal{A}_T \epsilon_{\alpha\beta\rho\sigma} n_+^\alpha n_-^\beta \epsilon_T^\rho \epsilon_{3T}^\sigma, \tag{40}$$

where A_L is the longitudinally polarized decay amplitude, and A_N and A_T are the transversely polarized contributions. Therefore, the total decay amplitude for $B_{(s)} \to (\bar{D}^*, D^*) \times [\phi, f_2^{(\prime)} \to]KK$ decays can be expressed as

$$|\mathcal{A}_{P(D)}|^2 = |\mathcal{A}_0|^2 + |\mathcal{A}_\parallel|^2 + |\mathcal{A}_\perp|^2, \tag{41}$$

where $\mathcal{A}_0$, $\mathcal{A}_\parallel$, and $\mathcal{A}_\perp$ are defined as

$$\mathcal{A}_0 = \mathcal{A}_L, \qquad \mathcal{A}_\parallel = \sqrt{2}\mathcal{A}_N, \qquad \mathcal{A}_\perp = \sqrt{2}\mathcal{A}_T. \tag{42}$$

The polarization fractions f_λ with $\lambda = 0$, $\parallel$, and $\perp$ are described as

$$f_\lambda = \frac{|\mathcal{A}_\lambda|^2}{|\mathcal{A}_0|^2 + |\mathcal{A}_\parallel|^2 + |\mathcal{A}_\perp|^2}, \tag{43}$$

with the normalization relation $f_0 + f_\parallel + f_\perp = 1$.

III. CALCULATION OF DECAY AMPLITUDES IN PQCD APPROACH

In this section, we intend to calculate the relevant decay amplitudes. For the considered $B_{(s)} \to \bar{D}^{(*)}(R \to)KK$ decays, the analytic formulas for the corresponding decay amplitudes are of the following form:

(i) S-wave:

$$\mathcal{A}(B_s^0 \to \bar{D}^0(f_0 \to)K^+K^-) = \frac{G_F}{\sqrt{2}} V_{cb}^* V_{us}[a_2 F_{ef_0}^{LL} + C_2 M_{ef_0}^{LL}], \tag{44}$$

$$\mathcal{A}(B_s^0 \to \bar{D}^{*0}(f_0 \to)K^+K^-) = \frac{G_F}{\sqrt{2}} V_{cb}^* V_{us}[a_2 F_{ef_0}^{LL} + C_2 M_{ef_0}^{LL}]. \tag{45}$$

(ii) P-wave:

$$\mathcal{A}(B_s^0 \to \bar{D}^0(\phi \to)K^+K^-) = \frac{G_F}{\sqrt{2}} V_{cb}^* V_{us}[a_2 F_{e\phi}^{LL} + C_2 M_{e\phi}^{LL}], \tag{46}$$

$$\mathcal{A}_i(B_s^0 \to \bar{D}^{*0}(\phi \to)K^+K^-) = \frac{G_F}{\sqrt{2}} V_{cb}^* V_{us}[a_2 F_{e\phi,i}^{LL} + C_2 M_{e\phi,i}^{LL}]. \tag{47}$$

(iii) D-wave:

$$\mathcal{A}(B^0 \to \bar{D}^0(f_2^q \to)K^+K^-) = \frac{G_F}{\sqrt{2}} V_{cb}^* V_{ud}[a_2(F_{ef_2}^{LL} + F_{af_2}^{LL}) + C_2(M_{ef_2}^{LL} + M_{af_2}^{LL})], \tag{48}$$

$$\mathcal{A}(B_s^0 \to \bar{D}^0(f_2^q \to)K^+K^-) = \frac{G_F}{\sqrt{2}} V_{cb}^* V_{us}[a_2 F_{af_2}^{LL} + C_2 M_{af_2}^{LL}], \tag{49}$$

$$\mathcal{A}(B_s^0 \to \bar{D}^0(f_2^s \to)K^+K^-) = \frac{G_F}{\sqrt{2}} V_{cb}^* V_{us}[a_2 F_{ef_2}^{LL} + C_2 M_{ef_2}^{LL}], \tag{50}$$

$$\mathcal{A}_i(B^0 \to \bar{D}^{*0}(f_2^q \to)K^+K^-) = \frac{G_F}{\sqrt{2}} V_{cb}^* V_{ud}[a_2(F_{ef_2,i}^{LL} + F_{af_2,i}^{LL}) + C_2(M_{ef_2,i}^{LL,i} + M_{af_2,i}^{LL,i})], \tag{51}$$

$$\mathcal{A}_i(B_s^0 \to \bar{D}^{*0}(f_2^q \to)K^+K^-) = \frac{G_F}{\sqrt{2}} V_{cb}^* V_{us}[a_2 F_{af_2,i}^{LLi} + C_2 M_{af_2,i}^{LL}], \tag{52}$$

$$\mathcal{A}_i(B_s^0 \to \bar{D}^{*0}(f_2^s \to)K^+K^-) = \frac{G_F}{\sqrt{2}} V_{cb}^* V_{us}[a_2 F_{ef_2,i}^{LL} + C_2 M_{ef_2,i}^{LL}]. \tag{53}$$

While for $B_{(s)} \to D^{(*)}(R \to)KK$ channels, the total decay amplitudes are written as

(i) S-wave:

$$\mathcal{A}(B_s^0 \to D^0(f_0 \to)K^+K^-) = \frac{G_F}{\sqrt{2}} V_{ub}^* V_{cs}[a_2 F_{ef_0}^{LL} + C_2 M_{ef_0}^{LL}], \tag{54}$$

$$\mathcal{A}(B_s^0 \to D^{*0}(f_0 \to)K^+K^-) = \frac{G_F}{\sqrt{2}} V_{ub}^* V_{cs}[a_2 F_{ef_0}^{LL} + C_2 M_{ef_0}^{LL}]. \tag{55}$$

(ii) P-wave:

$$\mathcal{A}(B_s^0 \to D^0(\phi \to)K^+K^-) = \frac{G_F}{\sqrt{2}} V_{ub}^* V_{cs}[a_2 F_{e\phi}^{LL} + C_2 M_{e\phi}^{LL}], \tag{56}$$

$$\mathcal{A}_i(B_s^0 \to D^{*0}(\phi \to)K^+K^-) = \frac{G_F}{\sqrt{2}} V_{ub}^* V_{cs}[a_2 F_{e\phi,i}^{LL} + C_2 M_{e\phi,i}^{LL}]. \tag{57}$$

(iii) D-wave:

$$\mathcal{A}(B^+ \to D^+(f_2^q \to)K^+K^-) = \frac{G_F}{\sqrt{2}} V_{ub}^* V_{cd}[a_1(F_{ef_2}^{LL} + F_{aD}^{LL}) + C_1(M_{ef_2}^{LL} + M_{aD}^{LL})], \tag{58}$$

$$\mathcal{A}(B^0 \to D^0(f_2^q \to)K^+K^-) = \frac{G_F}{\sqrt{2}} V_{ub}^* V_{cd}[a_2(F_{ef_2}^{LL} + F_{aD}^{LL}) + C_2(M_{ef_2}^{LL} + M_{aD}^{LL})], \tag{59}$$

$$\mathcal{A}(B_s^0 \to D^0(f_2^q \to)K^+K^-) = \frac{G_F}{\sqrt{2}} V_{ub}^* V_{cs}[a_2 F_{aD}^{LL} + C_2 M_{aD}^{LL}], \tag{60}$$

$$\mathcal{A}(B_s^0 \to D^0(f_2^s \to)K^+K^-) = \frac{G_F}{\sqrt{2}} V_{ub}^* V_{cs}[a_2 F_{ef_2}^{LL} + C_2 M_{ef_2}^{LL}], \tag{61}$$

$$\mathcal{A}_i(B^+ \to D^{*+}(f_2^q \to)K^+K^-) = \frac{G_F}{\sqrt{2}} V_{ub}^* V_{cd}[a_1(F_{ef_2,i}^{LL} + F_{aD^*,i}^{LL}) + C_1(M_{ef_2,i}^{LL} + M_{aD^*,i}^{LL})], \tag{62}$$

$$\mathcal{A}_i(B^0 \to D^{*0}(f_2^q \to)K^+K^-) = \frac{G_F}{\sqrt{2}} V_{ub}^* V_{cd}[a_2(F_{ef_2,i}^{LL} + F_{aD^*,i}^{LL}) + C_2(M_{ef_2,i}^{LL} + M_{aD^*,i}^{LL})], \tag{63}$$

$$\mathcal{A}_i(B_s^0 \to D^{*0}(f_2^q \to)K^+K^-) = \frac{G_F}{\sqrt{2}} V_{ub}^* V_{cs}[a_2 F_{aD^*,i}^{LL} + C_2 M_{aD^*,i}^{LL}], \tag{64}$$

$$\mathcal{A}_i(B_s^0 \to D^{*0}(f_2^s \to)K^+K^-) = \frac{G_F}{\sqrt{2}} V_{ub}^* V_{cs}[a_2 F_{ef_2,i}^{LL} + C_2 M_{ef_2,i}^{LL}], \tag{65}$$

in which the combinations a_i of the Wilson coefficients are defined as

$$a_1 = C_2 + \frac{C_1}{3}, \qquad a_2 = C_1 + \frac{C_2}{3}. \tag{66}$$

For $B_{(s)} \to (\bar{D}^*, D^*)[\phi, f_2^{(\prime)} \to]KK$ decays, the superscripts $i = L, N, T$, represent longitudinal, parallel, and transverse polarization contributions respectively. $F_{e(a)}^{LL}$ and $M_{e(a)}^{LL}$ describe the contributions from the factorizable emission (annihilation) and nonfactorizable emission (annihilation) diagrams as show in Figs. 1 and 2. The explicit expressions of the amplitudes $F_{e(a)}^{LL}$ and $M_{e(a)}^{LL}$ will be given in the Appendix.

IV. NUMERICAL RESULTS

In this section, let us first list the parameters used in our numerical calculations, such as the masses (in units of GeV) [103]:

$$\begin{aligned} &m_B = 5.280, \quad m_{B_s} = 5.367, \quad m_b = 4.8, \quad m_c = 1.275, \quad m_{K^\pm} = 0.494, \\ &m_{D^\pm} = 1.870, \quad m_{D^0/\bar{D}^0} = 1.864, \quad m_{D^{*\pm}} = 2.010, \quad m_{D^{*0}/\bar{D}^{*0}} = 2.007. \end{aligned} \tag{67}$$

The values of the Wolfenstein parameters are adopted as given in Ref. [103]: $A = 0.836 \pm 0.015$, $\lambda = 0.22453 \pm 0.00044$, $\bar{\rho} = 0.122^{+0.018}_{-0.017}$, $\bar{\eta} = 0.355^{+0.012}_{-0.011}$.

The decay constants (in units of GeV) and the B meson lifetimes (in units of ps) are chosen as [56,123,124]

$$\begin{aligned} &f_B = 0.19 \pm 0.02, \quad f_{B_s} = 0.23 \pm 0.02, \quad f_{\phi(1020)} = 0.215, \quad f_{\phi(1020)}^T = 0.186, \\ &f_{f_2(1270)} = 0.102, \quad f_{f_2(1270)}^T = 0.117, \quad f_{f_2'(1525)} = 0.126, \quad f_{f_2'(1525)}^T = 0.065, \\ &\tau_{B^0} = 1.519, \quad \tau_{B^\pm} = 1.638, \quad \tau_{B_s} = 1.512. \end{aligned} \tag{68}$$

The form factor ratio r^T, the coefficients c_i, and the Gegenbauer moments $a_{S,P,D}$ have adopted the same values as those determined in Ref. [61],

$$
\begin{aligned}
r^T(\phi(1020)) &= 0.865, \quad r^T(\phi(1680)) = 0.6, \quad r^T(f_2(1270)) = 1.15,\\
r^T(f_2'(1525)) &= 0.52, \quad r^T(f_2(1750)) = 0.3, \quad r^T(f_2(1950)) = 1.5,\\
c_{f_0(1370)} &= 0.12e^{i\frac{\pi}{2}}, \quad c_{\phi(1680)} = 0.6, \quad c_{f_2'(1525)} = 1.2,\\
c_{f_2(1270)} &= 0.1e^{i\pi}, \quad c_{f_2(1750)} = 0.4e^{i\pi}, \quad c_{f_2(1950)} = 0.3,\\
a_S &= 0.80 \pm 0.16, \quad a_D^0 = 0.40 \pm 0.08, \quad a_D^T = 0.90 \pm 0.18,\\
a_{2P}^0 &= -0.50 \pm 0.10, \quad a_{2P}^s = -0.70 \pm 0.14, \quad a_{2P}^t = -0.30 \pm 0.06,\\
a_{2P}^T &= -0.50 \pm 0.10, \quad a_{2P}^a = 0.40 \pm 0.08, \quad a_{2P}^v = -0.60 \pm 0.12.
\end{aligned} \tag{69}
$$

By using the Eqs. (37)–(43), the decay amplitudes in Sec. III and the Appendix and all the input quantities, the resultant branching ratios $\mathcal{B}$ and the polarization fractions f_λ together with the available experimental measurements for the considered quasi-two-body decays $B_{(s)} \to [D^{(*)}, \bar{D}^{(*)}](R \to)KK$ are summarized in Tables II–VI. In our numerical calculations for the branching ratios and polarization fractions, the first theoretical uncertainty results from the parameters of the wave functions of the initial and final states, such as the shape parameter

TABLE II. PQCD results for the branching ratios of the S, P, and D wave resonance channels in the $B_{(s)}^0 \to \bar{D}K^+K^-$ decay together with experimental data [103]. The theoretical errors are attributed to the variation of the shape parameters $\omega_{B_{(s)}}(C_{\bar{D}})$ in the wave function of the $B_{(s)}(\bar{D})$ meson and the decay constant $f_{B_{(s)}}$, the Gegenbauer moments of two-kaon DAs, and the hard scale t and the QCD scale $\Lambda_{\rm QCD}$, respectively.

Decay modes		Quasi-two-body	Data [103]
$B_s^0 \to \bar{D}^0(f_0(980) \to)K^+K^-$	$\mathcal{B}(10^{-6})$	$1.36^{+0.61+0.67+0.79}_{-0.46-0.54-0.64}$	< 1.55
$B_s^0 \to \bar{D}^0(f_0(1370) \to)K^+K^-$	$\mathcal{B}(10^{-7})$	$5.66^{+2.68+2.70+3.18}_{-1.95-2.21-2.56}$	…
$B_s^0 \to \bar{D}^0(\phi(1020) \to)K^+K^-$	$\mathcal{B}(10^{-5})$	$1.21^{+0.51+0.23+0.90}_{-0.41-0.30-0.54}$	1.50 ± 0.25
$B_s^0 \to \bar{D}^0(\phi(1680) \to)K^+K^-$	$\mathcal{B}(10^{-6})$	$1.35^{+0.67+0.24+1.10}_{-0.48-0.23-0.72}$	…
$B_s^0 \to \bar{D}^0(f_2(1270) \to)K^+K^-$	$\mathcal{B}(10^{-7})$	$1.87^{+0.49+0.79+0.35}_{-0.47-0.69-0.62}$	…
$B_s^0 \to \bar{D}^0(f_2'(1525) \to)K^+K^-$	$\mathcal{B}(10^{-6})$	$3.56^{+1.42+1.57+1.94}_{-1.12-1.28-1.62}$	…
$B_s^0 \to \bar{D}^0(f_2(1750) \to)K^+K^-$	$\mathcal{B}(10^{-7})$	$2.76^{+1.17+1.22+1.46}_{-0.90-0.99-1.18}$	…
$B_s^0 \to \bar{D}^0(f_2(1950) \to)K^+K^-$	$\mathcal{B}(10^{-8})$	$7.02^{+2.36+3.10+3.66}_{-2.01-2.52-3.91}$	…
$B^0 \to \bar{D}^0(f_2(1270) \to)K^+K^-$	$\mathcal{B}(10^{-6})$	$3.54^{+1.60+1.55+1.20}_{-1.45-1.28-1.15}$	…
$B^0 \to \bar{D}^0(f_2'(1525) \to)K^+K^-$	$\mathcal{B}(10^{-8})$	$5.86^{+5.57+3.97+2.68}_{-1.53-1.49-1.90}$	…

TABLE III. PQCD results for the branching ratios of the S, P, and D wave resonance channels in the $B_{(s)}^0 \to \bar{D}^*K^+K^-$ decay together with experimental data [103]. The theoretical errors are attributed to the variation of the shape parameters $\omega_{B_{(s)}}(C_{\bar{D}^*})$ in the wave function of the $B_{(s)}(\bar{D}^*)$ meson and the decay constant $f_{B_{(s)}}$, the Gegenbauer moments of two-kaon DAs, and the hard scale t and the QCD scale $\Lambda_{\rm QCD}$, respectively.

Decay modes		Quasi-two-body	Data [103]
$B_s^0 \to \bar{D}^{*0}(f_0(980) \to)K^+K^-$	$\mathcal{B}(10^{-6})$	$1.14^{+0.52+0.56+0.66}_{-0.37-0.44-0.50}$	…
$B_s^0 \to \bar{D}^{*0}(f_0(1370) \to)K^+K^-$	$\mathcal{B}(10^{-7})$	$4.66^{+2.29+2.23+2.78}_{-1.55-1.82-2.09}$	…
$B_s^0 \to \bar{D}^{*0}(\phi(1020) \to)K^+K^-$	$\mathcal{B}(10^{-5})$	$1.76^{+0.64+0.22+0.92}_{-0.51-0.18-0.70}$	1.85 ± 0.30
$B_s^0 \to \bar{D}^{*0}(\phi(1680) \to)K^+K^-$	$\mathcal{B}(10^{-6})$	$2.11^{+0.90+0.27+0.98}_{-0.66-0.19-0.66}$	…
$B_s^0 \to \bar{D}^{*0}(f_2(1270) \to)K^+K^-$	$\mathcal{B}(10^{-7})$	$2.45^{+0.67+0.95+0.25}_{-0.56-0.78-0.31}$	…
$B_s^0 \to \bar{D}^{*0}(f_2'(1525) \to)K^+K^-$	$\mathcal{B}(10^{-6})$	$6.99^{+2.91+2.24+1.77}_{-2.19-1.81-1.35}$	…
$B_s^0 \to \bar{D}^{*0}(f_2(1750) \to)K^+K^-$	$\mathcal{B}(10^{-7})$	$6.25^{+2.54+2.04+1.21}_{-1.98-1.66-0.99}$	…
$B_s^0 \to \bar{D}^{*0}(f_2(1950) \to)K^+K^-$	$\mathcal{B}(10^{-7})$	$3.55^{+1.22+1.26+1.10}_{-1.05-1.03-0.74}$	…
$B^0 \to \bar{D}^{*0}(f_2(1270) \to)K^+K^-$	$\mathcal{B}(10^{-5})$	$3.67^{+1.21+1.42+0.66}_{-1.01-1.15-0.58}$	…
$B^0 \to \bar{D}^{*0}(f_2'(1525) \to)K^+K^-$	$\mathcal{B}(10^{-7})$	$5.76^{+1.81+2.17+0.84}_{-1.57-1.77-0.59}$	…

TABLE IV. PQCD results for the branching ratios of the S, P, and D wave resonance channels in the $B_{(s)} \to DK^+K^-$ decay. The theoretical errors are attributed to the variation of the shape parameters $\omega_{B_{(s)}}(C_D)$ in the wave function of $B_{(s)}(D)$ meson and the decay constant $f_{B_{(s)}}$, the Gegenbauer moments of two-kaon DAs, and the hard scale t and the QCD scale $\Lambda_{\rm QCD}$, respectively.

Decay modes		Quasi-two-body
$B_s^0 \to D^0(f_0(980) \to)K^+K^-$	$\mathcal{B}(10^{-7})$	$1.30^{+0.62+0.58+0.31}_{-0.46-0.46-0.45}$
$B_s^0 \to D^0(f_0(1370) \to)K^+K^-$	$\mathcal{B}(10^{-8})$	$3.91^{+1.54+1.89+0.48}_{-1.26-1.46-1.10}$
$B_s^0 \to D^0(\phi(1020) \to)K^+K^-$	$\mathcal{B}(10^{-7})$	$9.65^{+3.64+4.05+2.03}_{-3.69-4.23-3.88}$
$B_s^0 \to D^0(\phi(1680) \to)K^+K^-$	$\mathcal{B}(10^{-8})$	$7.42^{+4.32+4.27+2.49}_{-2.79-3.18-2.61}$
$B_s^0 \to D^0(f_2(1270) \to)K^+K^-$	$\mathcal{B}(10^{-8})$	$7.23^{+1.90+3.19+1.09}_{-1.58-2.60-1.37}$
$B_s^0 \to D^0(f_2'(1525) \to)K^+K^-$	$\mathcal{B}(10^{-7})$	$4.39^{+2.04+1.94+1.17}_{-1.53-1.58-1.54}$
$B_s^0 \to D^0(f_2(1750) \to)K^+K^-$	$\mathcal{B}(10^{-8})$	$2.29^{+2.12+1.74+1.47}_{-0.39-0.50-0.49}$
$B_s^0 \to D^0(f_2(1950) \to)K^+K^-$	$\mathcal{B}(10^{-8})$	$4.07^{+1.63+1.79+0.60}_{-1.28-1.47-1.20}$
$B^+ \to D^+(f_2(1270) \to)K^+K^-$	$\mathcal{B}(10^{-7})$	$1.76^{+0.44+0.78+0.10}_{-0.40-0.63-0.22}$
$B^+ \to D^+(f_2'(1525) \to)K^+K^-$	$\mathcal{B}(10^{-9})$	$1.05^{+0.25+0.46+0.02}_{-0.24-0.38-0.15}$
$B^0 \to D^0(f_2(1270) \to)K^+K^-$	$\mathcal{B}(10^{-8})$	$1.66^{+0.56+0.73+0.16}_{-0.45-0.60-0.28}$
$B^0 \to D^0(f_2'(1525) \to)K^+K^-$	$\mathcal{B}(10^{-10})$	$1.52^{+0.48+0.67+0.16}_{-0.37-0.54-0.29}$

TABLE V. PQCD results for the branching ratios of the S, P, and D wave resonance channels in the $B_{(s)} \to D^*K^+K^-$ decay. The theoretical errors are attributed to the variation of the shape parameters $\omega_{B_{(s)}}(C_{D^*})$ in the wave function of the $B_{(s)}(D^*)$ meson and the decay constant $f_{B_{(s)}}$, the Gegenbauer moments of two-kaon DAs, and the hard scale t and the QCD scale $\Lambda_{\rm QCD}$, respectively.

Decay modes		Quasi-two-body
$B_s^0 \to D^{*0}(f_0(980) \to)K^+K^-$	$\mathcal{B}(10^{-8})$	$9.67^{+4.23+3.21+2.23}_{-3.40-2.81-3.17}$
$B_s^0 \to D^{*0}(f_0(1370) \to)K^+K^-$	$\mathcal{B}(10^{-8})$	$3.06^{+1.13+1.13+0.46}_{-1.00-0.97-0.81}$
$B_s^0 \to D^{*0}(\phi(1020) \to)K^+K^-$	$\mathcal{B}(10^{-7})$	$6.39^{+1.73+0.93+0.07}_{-2.90-2.64-3.46}$
$B_s^0 \to D^{*0}(\phi(1680) \to)K^+K^-$	$\mathcal{B}(10^{-8})$	$4.69^{+2.83+2.01+1.18}_{-1.66-1.82-1.54}$
$B_s^0 \to D^{*0}(f_2(1270) \to)K^+K^-$	$\mathcal{B}(10^{-8})$	$3.12^{+0.67+1.18+0.62}_{-0.64-0.96-0.89}$
$B_s^0 \to D^{*0}(f_2'(1525) \to)K^+K^-$	$\mathcal{B}(10^{-7})$	$4.01^{+1.61+1.64+0.79}_{-1.43-1.34-1.13}$
$B_s^0 \to D^{*0}(f_2(1750) \to)K^+K^-$	$\mathcal{B}(10^{-8})$	$2.22^{+1.11+0.93+0.65}_{-0.80-0.77-0.66}$
$B_s^0 \to D^{*0}(f_2(1950) \to)K^+K^-$	$\mathcal{B}(10^{-8})$	$4.87^{+1.93+1.81+0.61}_{-1.49-1.49-1.09}$
$B^+ \to D^{*+}(f_2(1270) \to)K^+K^-$	$\mathcal{B}(10^{-7})$	$1.72^{+0.47+0.62+0.18}_{-0.42-0.51-0.20}$
$B^+ \to D^{*+}(f_2'(1525) \to)K^+K^-$	$\mathcal{B}(10^{-9})$	$1.06^{+0.24+0.36+0.10}_{-0.24-0.30-0.13}$
$B^0 \to D^{*0}(f_2(1270) \to)K^+K^-$	$\mathcal{B}(10^{-8})$	$1.10^{+0.36+0.38+0.17}_{-0.30-0.32-0.30}$
$B^0 \to D^{*0}(f_2'(1525) \to)K^+K^-$	$\mathcal{B}(10^{-11})$	$7.96^{+2.41+3.21+1.12}_{-2.11-2.61-2.61}$

$\omega_B = 0.40 \pm 0.04$ GeV or $\omega_{B_s} = 0.50 \pm 0.05$ GeV and $C_D = 0.5 \pm 0.1$, and the decay constant $f_{B_{(s)}}$ in a $B_{(s)}$ meson wave function. The second one is due to the Gegenbauer moments in DAs of a KK pair with different intermediate resonances, which are supposed to be varied with a 20% range for the error estimation. With the improvements of the experiments and the deeper theoretical developments, these kinds of uncertainties will be reduced. The last one is caused by the variation of the hard scale t from $0.75t$ to $1.25t$ (without changing $1/b_i$) and the QCD scale $\Lambda_{\rm QCD} = 0.25 \pm 0.05$ GeV, which characterizes the effect of the next-to-leading-order QCD contributions. The possible errors due to the uncertainties of m_c and CKM matrix elements are very small and can be neglected safely.

Compared with $B_{(s)} \to D^{(*)}R \to D^{(*)}KK$ decays, the $B_{(s)} \to \bar{D}^{(*)}R \to \bar{D}^{(*)}KK$ ones are enhanced by the CKM matrix elements $|V_{cb}/V_{ub}|^2$, especially for those without a strange quark in the four-quark operators. So for most of the $B_{(s)} \to \bar{D}^{(*)}R \to \bar{D}^{(*)}KK$ decays, the branching ratios are at the order from 10^{-7} to 10^{-5}; while for the $B_{(s)} \to D^{(*)}R \to D^{(*)}KK$ decays, the branching ratios are at the order from 10^{-9} to 10^{-7}. The two-body branching fraction $\mathcal{B}(B \to D^{(*)}R)$ can be extracted from the corresponding quasi-two-body decay modes in Tables II–V under the narrow width approximation relation

$$\mathcal{B}(B \to D^{(*)}R \to D^{(*)}K^+K^-) = \mathcal{B}(B \to D^{(*)}R) \cdot \mathcal{B}(R \to K^+K^-). \quad (70)$$

By using the measured branching fractions $\mathcal{B}(\phi(1020) \to K^+K^-) = 49.2\%$, $\mathcal{B}(f_2(1270) \to K^+K^-) = 2.3\%$ and $\mathcal{B}(f_2'(1525) \to K^+K^-) = 44.4\%$ [103] as an input, we can extract the branching ratios of two-body decays $B \to D^{(*)}\phi(1020)$, $B \to D^{(*)}f_2(1270)$, and $B \to D^{(*)}f_2'(1525)$, which agree with those from the two-body analyses based on the PQCD approach [23–25] within errors. The tiny differences between our predictions of the two-body decays and previous results of Refs. [23–25] are mainly due to the parametric origins and the power corrections related to the ratio $r_D^2 = m_D^2/m_B^2$. As we know, a significant impact of nonfactorizable contribution is expected for a color suppressed decay mode. Taking the decay channel $B_s^0 \to \bar{D}^{*0}(\phi(1020) \to)K^+K^-$ as an example, one can see that the inclusion of the power correction r_D^2 can suppress the branching ratio efficiently, especially for the contributions of nonfactorizable emission diagrams as shown in Table VII.

Now, we come to discuss the contributions of P-wave resonances. It is obvious that the PQCD predictions of the $\mathcal{B}(B_s^0 \to \bar{D}^{(*)0}\phi(1020) \to \bar{D}^{(*)0}K^+K^-)$ are consistent well with the experimental data within errors. Taking the $B_s^0 \to \bar{D}^0K^+K^-$ decay as an example, we can calculate the total P-wave resonance contributions $\mathcal{B}(B_s^0 \to \bar{D}^0K^+K^-)_{P\text{-wave}} = 1.32 \times 10^{-5}$, which is nearly equal to the sum of resonance contributions from $\phi(1020)$ and $\phi(1680)$. The main reason is that the interference between the two P-wave resonant states $\phi(1020)$ and $\phi(1680)$ is really small due to the rather narrow width of the former ($\Gamma_{\phi(1020)} = 4.25$ MeV). Since the contribution from high mass resonance is one order of magnitude smaller, the P-wave resonance contribution is dominant by $\phi(1020)$. From the numerical results given in Tables II and III, we

TABLE VI. PQCD results for the polarization fractions of the $B_{(s)} \to (\bar{D}^*, D^*)[\phi, f_2^{(\prime)} \to]K^+K^-$ decays together with experimental data [103]. The theoretical errors are attributed to the variation of the shape parameters $\omega_{B_{(s)}}(C_{D^*})$ in the wave function of the $B_{(s)}(D^*)$ meson and the decay constant $f_{B_{(s)}}$, the Gegenbauer moments of two-kaon DAs, and the hard scale t and the QCD scale $\Lambda_{\rm QCD}$, respectively.

Decay modes	$f_0(\%)$	$f_\parallel(\%)$	$f_\perp(\%)$
$B_s^0 \to \bar{D}^{*0}(\phi(1020) \to)K^+K^-$	$54.7^{+1.4+5.2+12.7}_{-2.2-5.4-17.0}$	$34.4^{+1.6+3.7+13.6}_{-1.4-4.0-10.0}$	$10.9^{+0.6+3.1+3.5}_{-0.0-2.2-2.8}$
Data [103]	$73 \pm 15 \pm 4$	...	...
$B_s^0 \to \bar{D}^{*0}(\phi(1680) \to)K^+K^-$	$45.9^{+1.7+5.9+14.1}_{-1.8-5.3-15.2}$	$39.1^{+1.6+3.9+13.0}_{-1.3-4.3-10.9}$	$14.9^{+0.3+2.7+2.8}_{-0.2-2.6-3.1}$
$B_s^0 \to \bar{D}^{*0}(f_2(1270) \to)K^+K^-$	$12.9^{+1.9+7.6+0.9}_{-1.6-5.5-1.4}$	$34.2^{+0.6+2.1+1.5}_{-0.8-3.1-2.8}$	$52.9^{+1.2+3.3+2.0}_{-1.9-4.6-1.0}$
$B_s^0 \to \bar{D}^{*0}(f_2'(1525) \to)K^+K^-$	$38.8^{+1.9+14.1+11.8}_{-1.7-12.9-12.2}$	$29.1^{+0.8+6.1+6.6}_{-0.9-6.7-5.9}$	$32.1^{+0.9+6.7+5.7}_{-1.2-7.5-5.9}$
$B_s^0 \to \bar{D}^{*0}(f_2(1750) \to)K^+K^-$	$34.7^{+1.5+13.6+10.7}_{-1.6-12.2-11.1}$	$31.6^{+0.8+5.8+5.8}_{-0.8-6.7-5.4}$	$33.8^{+0.7+6.2+5.2}_{-0.9-7.2-5.6}$
$B_s^0 \to \bar{D}^{*0}(f_2(1950) \to)K^+K^-$	$23.5^{+2.7+11.4+14.0}_{-3.8-9.2-10.3}$	$35.8^{+1.5+4.3+5.5}_{-1.2-5.4-7.1}$	$40.7^{+2.3+5.0+4.8}_{-1.5-6.0-7.0}$
$B^0 \to \bar{D}^{*0}(f_2(1270) \to)K^+K^-$	$13.4^{+1.8+7.6+9.2}_{-1.7-5.7-7.5}$	$37.8^{+1.0+2.5+3.2}_{-1.0-3.3-3.9}$	$48.8^{+0.7+3.3+4.3}_{-0.8-4.3-5.3}$
$B^0 \to \bar{D}^{*0}(f_2'(1525) \to)K^+K^-$	$16.1^{+2.2+8.9+8.4}_{-2.5-6.7-7.1}$	$32.2^{+1.1+2.6+3.1}_{-0.9-3.4-3.2}$	$51.7^{+1.4+4.2+4.1}_{-1.4-5.5-5.1}$
$B_s^0 \to D^{*0}(\phi(1020) \to)K^+K^-$	$79.6^{+1.6+5.2+1.9}_{-2.8-12.6-6.2}$	$13.5^{+2.3+8.1+2.1}_{-3.1-3.6-3.2}$	$6.9^{+1.5+4.9+4.2}_{-0.0-2.2-0.0}$
$B_s^0 \to D^{*0}(\phi(1680) \to)K^+K^-$	$75.6^{+1.8+9.5+1.9}_{-1.2-14.5-11.2}$	$8.9^{+0.6+5.3+8.2}_{-0.4-3.5-0.4}$	$15.5^{+0.8+9.2+3.0}_{-1.4-6.0-1.8}$
$B_s^0 \to D^{*0}(f_2(1270) \to)K^+K^-$	$84.2^{+0.2+6.7+1.8}_{-0.3-8.8-2.8}$	$9.1^{+0.2+5.1+1.4}_{-0.0-3.8-1.1}$	$6.7^{+0.1+3.7+1.5}_{-0.2-2.8-0.9}$
$B_s^0 \to D^{*0}(f_2'(1525) \to)K^+K^-$	$92.6^{+0.7+3.4+2.5}_{-0.3-4.7-1.7}$	$3.9^{+0.2+2.6+0.8}_{-0.3-1.7-1.1}$	$3.5^{+0.3+2.1+0.7}_{-0.5-1.7-1.4}$
$B_s^0 \to D^{*0}(f_2(1750) \to)K^+K^-$	$95.5^{+0.8+2.1+1.5}_{-0.3-2.9-2.2}$	$2.2^{+0.3+1.3+2.3}_{-1.1-1.1-3.6}$	$2.3^{+0.3+1.6+0.9}_{-0.2-1.0-0.3}$
$B_s^0 \to D^{*0}(f_2(1950) \to)K^+K^-$	$83.2^{+0.6+7.1+3.6}_{-0.5-9.0-1.8}$	$9.1^{+0.6+5.1+0.9}_{-0.3-3.8-1.6}$	$7.6^{+0.1+4.1+0.8}_{-0.2-3.1-1.8}$
$B^+ \to D^{*+}(f_2(1270) \to)K^+K^-$	$79.3^{+0.1+8.3+1.1}_{-0.1-10.7-0.6}$	$11.9^{+0.1+6.2+1.1}_{-0.1-4.8-1.0}$	$8.8^{+0.1+4.6+0.1}_{-0.0-3.5-0.7}$
$B^+ \to D^{*+}(f_2'(1525) \to)K^+K^-$	$72.9^{+2.3+10.3+1.0}_{-1.4-12.4-1.7}$	$16.1^{+1.0+7.5+1.5}_{-1.2-6.1-0.0}$	$11.0^{+0.4+5.0+1.4}_{-1.2-4.2-2.4}$
$B^0 \to D^{*0}(f_2(1270) \to)K^+K^-$	$75.4^{+1.0+9.5+4.0}_{-0.7-11.8-1.2}$	$14.2^{+0.4+6.8+0.8}_{-0.2-5.5-2.0}$	$10.4^{+0.3+5.0+0.3}_{-0.8-4.0-2.0}$
$B^0 \to D^{*0}(f_2'(1525) \to)K^+K^-$	$90.8^{+0.7+4.2+3.6}_{-0.9-5.6-2.7}$	$3.0^{+0.5+1.8+1.5}_{-0.0-1.3-1.7}$	$6.2^{+0.6+3.8+1.2}_{-0.5-2.8-2.3}$

obtain the relative ratio $R(\phi)$ between the branching ratio of the B_s^0 meson into $\bar{D}^{*0}$ and $\bar{D}^0$ plus the resonance ϕ,

$$R^{\rm PQCD}(\phi) = \frac{\mathcal{B}(B_s^0 \to \bar{D}^{*0}(\phi \to)K^+K^-)}{\mathcal{B}(B_s^0 \to \bar{D}^0(\phi \to)K^+K^-)} = 1.45^{+1.28}_{-1.06}, \tag{71}$$

which is in agreement with the corresponding ratio of ϕ reported by the LHCb measurement [18],

$$R^{\rm exp}(\phi) = \frac{\mathcal{B}(B_s^0 \to \bar{D}^{*0}(\phi \to)K^+K^-)}{\mathcal{B}(B_s^0 \to \bar{D}^0(\phi \to)K^+K^-)} = 1.23 \pm 0.20 \pm 0.08, \tag{72}$$

where the first uncertainty is statistical and the second is systematic.

Utilizing the PQCD prediction in Table II and $\mathcal{B}(B_s^0 \to \bar{D}^0\bar{K}^{*0})) = (2.33^{+1.18}_{-0.69}) \times 10^{-4}$ taken from our previous work in Ref. [59] together with the two known branching ratios $\mathcal{B}(\phi \to K^+K^-) = (49.2 \pm 0.5)\%$ and $\mathcal{B}(K^* \to K\pi) \sim 100\%$ [103], we expect that

$$R^{\rm PQCD}_{\phi/\bar{K}^{*0}} = \frac{\mathcal{B}(B_s^0 \to \bar{D}^0\phi)}{\mathcal{B}(B_s^0 \to \bar{D}^0\bar{K}^{*0})} = 0.11^{+0.09}_{-0.07}, \tag{73}$$

which is a bit larger than the data measured by LHCb [14],

$$R^{\rm exp}_{\phi/\bar{K}^{*0}} = \frac{\mathcal{B}(B_s^0 \to \bar{D}^0\phi)}{\mathcal{B}(B_s^0 \to \bar{D}^0\bar{K}^{*0})} = 0.069 \pm 0.013({\rm stat}) \pm 0.007({\rm syst}). \tag{74}$$

TABLE VII. Branching fractions with (and without) the r_D^2-dependent terms in the $B_s^0 \to \bar{D}^{*0}(\phi(1020) \to)K^+K^-$ decays. FE and NFE represent the contributions from factorizable emission and nonfactorizable emission diagrams, respectively.

	FE $\mathcal{B}$ (in 10^{-7})			NFE $\mathcal{B}$ (in 10^{-5})			Total (in 10^{-5})
Modes	$\rm BR_L$	$\rm BR_N$	$\rm BR_T$	$\rm BR_L$	$\rm BR_N$	$\rm BR_T$	Br
$B_s^0 \to \bar{D}^{*0}(\phi(1020) \to)K^+K^-$	0.26	1.32	0.04	1.35	0.66	0.24	2.26
$B_s^0 \to \bar{D}^{*0}(\phi(1020) \to)K^+K^-(r_D^2)$	0.27	1.04	0.16	0.95	0.53	0.18	1.76

Recalling that the theoretical errors are relatively large, one still can count them as being consistent within one standard deviation.

In contrast to the vector resonances, the identification of the scalar mesons is a long-standing puzzle. Scalar resonances are difficult to resolve because some of them have large decay widths, which cause a strong overlap between resonances and background. The prominent appearance of the $f_0(980)$ implies a dominant $(\bar{s}s)$ component in the semileptonic D_s decays and decays of $B_{(s)}$ mesons. By assuming the $f_0(980)$ as a pure $\bar{s}s$ state, the authors studied the $B_s \to J/\psi f_0(980)$ by using the light-cone QCD sum rule and factorization assumption in Ref. [125] and using generalized factorization and SU(3) flavor symmetry in Ref. [126]. In Ref. [127], the authors calculated the $\bar{B}_s \to f_0(980)$ form factor from the light-cone sum rules with B-meson DAs, and investigated the S-wave $\bar{B}_s \to KK$ form factors to study the width effect, where the $f_0(980)$ is dominated by the $\bar{s}s$ configuration. Ratios of decay rates of B and/or B_s mesons into J/ψ plus $f_0(980)$ or $f_0(500)$ were proposed to allow for an extraction of the flavor mixing angle and to probe the tetraquark nature of those mesons within a certain model [128,129]. The phenomenological fits of the LHCb Collaboration neither allow for a contribution of the $f_0(980)$ in the $B \to J/\psi\pi\pi$ [121] nor an $f_0(500)$ in $B_s \to J/\psi\pi\pi$ decays [120] by using the isobar model. The authors conclude that their data is incompatible with a model where $f_0(980)$ is formed from two quarks and two antiquarks (tetraquarks) at the eight standard deviation level. In addition, they extract an upper limit for the mixing angle of 17° at 90% confidence level between the $f_0(980)$ and the $f_0(500)$ that would correspond to a substantial $(\bar{s}s)$ content in $f_0(980)$ [121]. However, a substantial $f_0(980)$ contribution is also found in the B-decays in a dispersive analysis of the same data that allows for a model-independent inclusion of the hadronic final state interactions in Ref. [130], which puts into question the conclusions of Ref. [121]. At this stage, the quark structure of scalar particles are still quite controversial. As a first approximation, the S-wave timelike form factor $F_S(m^2_{KK})$ used to parametrize the S-wave two-kaon distribution amplitude has been determined in Ref. [61]. Therefore, we take into account $f_0(980)$ and $f_0(1370)$ in the $\bar{s}s$ density operator.

For the S-wave resonances $f_0(980)$ and $f_0(1370)$, first we define the ratio between the $f_0(980) \to K^+K^-$ and $f_0(980) \to \pi^+\pi^-$,

$$R_{K/\pi} = \frac{\mathcal{B}(B_s^0 \to \bar{D}^0 f_0(980)(\to K^+K^-))}{\mathcal{B}(B_s^0 \to \bar{D}^0 f_0(980)(\to \pi^+\pi^-))} \approx \frac{\mathcal{B}(f_0(980) \to K^+K^-)}{\mathcal{B}(f_0(980) \to \pi^+\pi^-)}. \quad (75)$$

On the experimental side, *BABAR* measured the ratio of the partial decay width of $f_0(980) \to K^+K^-$ to $f_0(980) \to \pi^+\pi^-$ of $R^{\rm exp}_{K/\pi} = 0.69 \pm 0.32$ using $B \to KK^+K^-$ and $B \to K\pi^+\pi^-$ decays [131]. Meanwhile, BES performed a partial wave analysis of $\chi_{c0} \to f_0(980)f_0(980) \to \pi^+\pi^-\pi^+\pi^-$ and $\chi_{c0} \to f_0(980)f_0(980) \to \pi^+\pi^-K^+K^-$ in $\psi(2S) \to \gamma\chi_{c0}$ decay and extracted the ratio as $R^{\rm exp}_{K/\pi} = 0.25^{+0.17}_{-0.11}$ [132,133]. Their average yielded $R^{\rm exp}_{K/\pi} = 0.35^{+0.15}_{-0.14}$ [16]. Recently, the LHCb Collaboration [15] reported a measurement, $\mathcal{B}(B_s^0 \to \bar{D}^0 f_0(980) \to \bar{D}^0\pi^+\pi^-) = (1.7 \pm 1.1) \times 10^{-6}$; one can roughly infer the wide range of $\mathcal{B}^{\rm exp}(B_s^0 \to \bar{D}^0 f_0(980) \to \bar{D}^0K^+K^-) = (0.2 - 1.0) \times 10^{-6}$ combining with the ratio $R^{\rm exp}_{K/\pi}$. Our PQCD prediction $\mathcal{B}(B_s^0 \to \bar{D}^0 f_0(980) \to \bar{D}^0K^+K^-) = (1.36^{+1.20}_{-0.96}) \times 10^{-6}$ lies above the range within errors, which also agrees with the upper limit 1.55×10^{-6} given by PDG [103] as shown in Table II. However, BES also measured $R_{K/\pi} = 0.625 \pm 0.21$ by studying the decays $J/\psi \to \phi f_0(980) \to \phi\pi^+\pi^-$ and $J/\psi \to \phi f_0(980) \to \phi K^+K^-$ in Ref. [134]. It seems that we hardly can reach a reliable and universal $R_{K/\pi}$. It should be stressed that there are large uncertainties in both experimental measurements and the theoretical calculations, so the discrepancy between the data and the theoretical results could be clarified with the high precision experimental data and the high precision of theoretical calculations. Since the situation of the knowledge about the $f_0(1370)$ decaying into KK or $\pi\pi$ is rather unclear, no evidence of the $f_0(1370)$ resonance in the $B \to DKK$ decay has been reported so far. Our predictions on the KK channel involving the scalar resonances $f_0(980)$ and $f_0(1370)$ in Tables II–V will be investigated at the ongoing LHCb and Belle-II experiments in the future.

The branching ratios of the considered D-wave resonances are also presented in Tables II–V. Belle [10] provided a Dalitz plot analysis of $\bar{B}^0 \to D^0\pi^+\pi^-$ decays and obtained the branching ratio of $\mathcal{B}(\bar{B}^0 \to D^0 f_2) = (1.20 \pm 0.18(\text{stat}) \pm 0.21(\text{syst})) \times 10^{-4}$. Afterwards, LHCb [16] analyzed the resonant substructures of $B^0 \to \bar{D}^0\pi^+\pi^-$ decays and reported the branching ratio of $\mathcal{B}(B^0 \to \bar{D}^0 f_2) = (1.68 \pm 0.11(\text{stat}) \pm 0.21(\text{syst})) \times 10^{-4}(\text{Isobar})$. Their weighted average yielded $\mathcal{B}(B^0 \to \bar{D}^0 f_2) = (1.56 \pm 0.21) \times 10^{-4}$ [103]. For a more direct comparison, we can extract out the branching fraction for the two-body decay $\mathcal{B}(B^0 \to \bar{D}^0 f_2) = (1.54^{+1.08}_{-0.97}) \times 10^{-4}$ through the narrow-width approximation relation in Eq. (70), which agrees with the above experimental results within uncertainties. Furthermore, we have explicitly written the relative ratio of $\mathcal{B}(B_s^0 \to \bar{D}^0 f_2(1270)(\to K^+K^-))$ compared to $\mathcal{B}(B_s^0 \to \bar{D}^0 f_2(1270)(\to \pi^+\pi^-))$ in the narrow width limit,

$$R(f_2) = \frac{\mathcal{B}(B_s^0 \to \bar{D}^0 f_2(1270)(\to K^+K^-))}{\mathcal{B}(B_s^0 \to \bar{D}^0 f_2(1270)(\to \pi^+\pi^-))} \approx \frac{\mathcal{B}(f_2(1270) \to K^+K^-)}{\mathcal{B}(f_2(1270) \to \pi^+\pi^-)}. \quad (76)$$

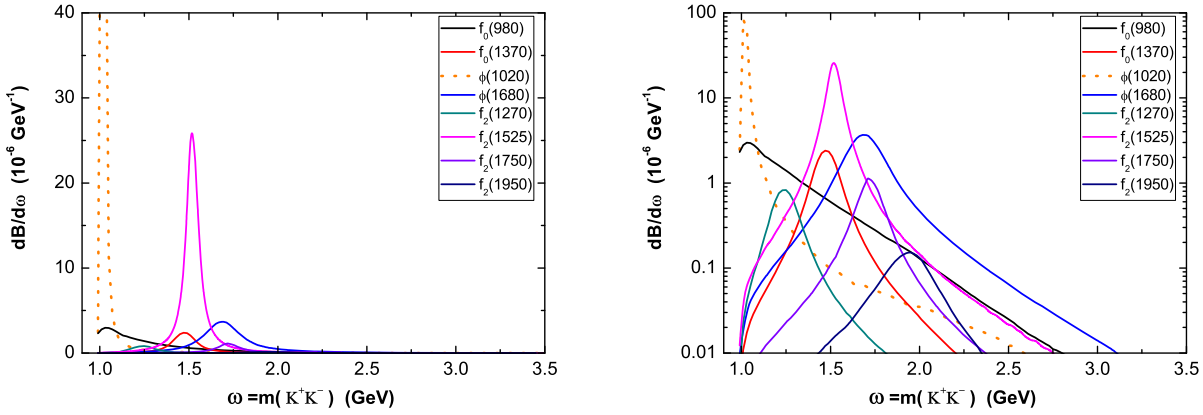

FIG. 3. (a) The $m(K^+K^-)$ dependence of the differential decay rates $d\mathcal{B}/d\omega$ for the contributions from the resonances $f_0(980)$, $f_0(1370)$, $\phi(1020)$, $\phi(1680)$, $f_2(1270)$, $f_2'(1525)$, $f_2(1750)$, and $f_2(1950)$ to $B_s^0 \to \bar{D}^0 K^+ K^-$ decay with a linear scale. (b) The same curves are shown with a logarithmic scale.

Thereby, using the experimental data $\mathcal{B}(f_2(1270) \to K^+K^-) = \frac{1}{2}(4.6)\%$, $\mathcal{B}(f_2(1270) \to \pi^+\pi^-) = \frac{2}{3}(84.2)\%$ from PDG [103] and the measurements $\mathcal{B}(B_s^0 \to \bar{D}^0 f_2(1270) \to \bar{D}^0\pi^+\pi^-) = (6.8 \pm 2.4) \times 10^{-5}$ from Belle [10] and $\mathcal{B}(B_s^0 \to \bar{D}^0 f_2(1270) \to \bar{D}^0\pi^+\pi^-) = (9.5 \pm 1.3) \times 10^{-5}$(Isobar) from LHCb [16], the experimental value of the $B_s^0 \to \bar{D}^0 f_2(1270)(\to K^+K^-)$ decay is estimated to be

$$\mathcal{B}(B_s^0 \to \bar{D}^0(f_2(1270) \to)K^+K^-) = \begin{cases} 2.7 \times 10^{-6}, & \text{Belle}, \\ 3.8 \times 10^{-6}, & \text{LHCb}, \end{cases}$$

which is one order of magnitude larger than our prediction $\mathcal{B}(B_s^0 \to \bar{D}^0 f_2(1270) \to \bar{D}^0 K^+K^-) = 1.87 \times 10^{-7}$ in its central value. Since the property of the tensor resonance is not well understood and the theoretical uncertainties are relatively large, this issue needs to be further clarified in the future.

From the numerical results given in Table II, we can evaluate the relative branching ratios between two tensor modes,

$$R_{f_2/f_2'} = \frac{\mathcal{B}(B_s^0 \to \bar{D}^0 f_2(1270))}{\mathcal{B}(B_s^0 \to \bar{D}^0 f_2'(1525))} = 0.05^{+0.10}_{-0.03}, \quad (77)$$

which can be tested by the forthcoming LHCb and Belle-II experiments.

In Fig. 3, we show the ω dependence of the differential decay rate $d\mathcal{B}(B_s^0 \to \bar{D}^0 K^+K^-)/d\omega$ after the inclusion of the possible contributions from the resonant states $f_0(980)$ (the black solid curve), $f_0(1370)$ (the red solid curve), $\phi(1020)$ (the orange dotted curve), $\phi(1680)$ (the blue solid curve), $f_2(1270)$ (the cyan solid curve), $f_2'(1525)$ (the magenta solid curve), $f_2(1750)$ (the violet solid curve), and $f_2(1950)$ (the navy solid curve). To see clearly all the peaks of the various resonances, we draw them both in Fig. 3(a) with a linear scale and Fig. 3(b) with a logarithmic one. For the considered decay mode $B_s^0 \to \bar{D}^0 K^+K^-$, the dynamical limit on the value of invariant mass ω is $(m_{K^+} + m_{K^-}) \leq \omega \leq (m_B - m_D)$. It is clear that an appreciable peak arises from the $\phi(1020)$ resonance, followed by $f_2'(1525)$. Another three resonance peaks of $f_0(980)$, $f_0(1370)$, and $\phi(1680)$ have relatively smaller strength than the $f_2'(1525)$ one, while their broader widths compensate the integrated strength over the whole phase space. Therefore, the branching ratios of the four components are of a comparable size as predicted in our work. The contribution of the tensor $f_2(1270)$ is really small in the $B_s^0 \to \bar{D}^0 K^+K^-$ decay mode, since it decays predominantly into $\pi\pi$. Apart from the above obvious signal peak, there are two visible structures at about 1750 and 1950 MeV in Fig. 3(b). Obviously, the differential branching ratios of these decays exhibit peaks at the pole mass of the resonant states. Thus, the main portion of the branching ratio lies in the region around the resonance as expected. For $B_s^0 \to \bar{D}^0\phi \to \bar{D}^0 K^+K^-$ decay, the central values of the branching ratio $\mathcal{B}$ are 5.82×10^{-6} and 8.29×10^{-6} when the integration over ω is limited in the range of $\omega = [m_\phi - 0.5\Gamma_\phi, m_\phi + 0.5\Gamma_\phi]$ or $\omega = [m_\phi - \Gamma_\phi, m_\phi + \Gamma_\phi]$ respectively, which amount to 48.1% and 68.5% of the total branching ratio $\mathcal{B} = 1.21 \times 10^{-5}$ as listed in Table II.

The $B \to (\bar{D}^*, D^*)[\phi, f_2^{(\prime)} \to]K^+K^-$ decays are vector-vector (vector-tensor) modes and can proceed through different polarization amplitudes. We display the polarization fractions associated with the available data in Table VI, which have the same origin of theoretical uncertainties as the branching ratios. It is easy to see that the fraction of the longitudinal polarization can be generally reduced to about ~50%, while the parallel and perpendicular ones are

roughly equal. The results are quite different from the expectation in the factorization assumption that the longitudinal polarization should dominate based on the quark helicity analysis [135,136]. For $B_s^0 \to \bar{D}^{*0}(\phi(1020)\to)K^+K^-$ decay, although the central value of $f_0 \approx 55\%$ is a little smaller than the measured one $f_0^{\rm exp} = 73\%$, they are consistent with each other due to the still large theoretical and experimental uncertainties.

It is worthwhile to stress that the polarization fractions of the color-suppressed decays $B \to \bar{D}^*(f_2\to)KK$ and $B \to D^*(f_2\to)KK$ are quite different from each other. For $B \to \bar{D}^*(f_2\to)KK$ ($\bar{b}\to\bar{c}$ transition) decays, the percentage of the transverse polarizations ($f_\parallel + f_\perp$) can be as large as 80%, while for $B \to D^*(f_2\to)KK$ ($\bar{b}\to\bar{u}$ transition) decays, the percentage of the transverse polarizations are only at the range of $10\% \sim 20\%$. This situation can be understood as the following reasons [25]: The $\bar{D}^*$ meson in $B \to \bar{D}^*(f_2\to)KK$ decays is longitudinal polarized since the $\bar{c}$ quark and the u quark in the $\bar{D}^*$ meson produced through the $(V-A)$ current are right-handed and left-handed, respectively. Because the $\bar{c}$ quack is massive, the helicity of the $\bar{c}$ quark can flip easily from right handed to left handed. Thus, the $\bar{D}^*$ meson can be transversely polarized with the polarization $\lambda = -1$. The recoiled tensor meson can also be transversely polarized with the polarization $\lambda = -1$ due to the contribution of orbital angular momentum. Then the transverse polarized contribution in $B \to \bar{D}^*(f_2\to)KK$ decays can be sizable. While for the D^* meson, the $\bar{u}$ quark in the D^* meson is right handed and the c quark can flip from left handed to right handed, which makes the D^* meson transversely polarized with the polarization $\lambda = +1$. In order to have the same polarization with the D^* meson, the recoiled transversely polarized tensor meson needs contributions from both orbital angular momentum and spin, so the situation is symmetric. But the wave function of the tensor meson is asymmetric. Therefore, the transversely polarized contribution in $B \to D^*(f_2\to)KK$ is suppressed on account of Bose statistics. More precise measurements of such decay channels are expected to help us to test and improve our theoretical calculations.

V. CONCLUSION

In this work, we have performed a systematic analysis of various partial wave resonant contributions to three-body $B_{(s)} \to [D^{(*)}, \bar{D}^{(*)}]KK$ decays in the PQCD approach. For $B_s^0 \to [D^{(*)}, \bar{D}^{(*)}]K^+K^-$ decay modes, the dominant contributions are expected to be from P-wave resonance $\phi(1020)$ and D-wave resonance $f_2'(1525)$. Besides the two prominent components mentioned above, some significant resonant structures also exhibit in the K^+K^- invariant mass spectrum, like $f_0(980)$, $f_0(1370)$, and $\phi(1680)$. Such resonances have relatively smaller strength than the $f_2'(1525)$ resonance, but their broader widths compensate the integrated strength over the entire phase space. Since $\pi\pi$ is the dominant decay mode of $f_2(1270)$, the contribution of the tensor $f_2(1270)$ is indeed small. The whole pattern of $B_{(s)} \to [D^{(*)}, \bar{D}^{(*)}]KK$ decays will be confronted with the experimental data in the future.

Each partial wave contribution can be parametrized into the corresponding timelike form factor, which contains the final state interactions between the kaons in the resonant regions. The Flatté model for the $f_0(980)$ resonance and the Breit-Wigner formulas for other resonances have been adopted to parametrize the timelike form factors $F_{S,P,D}(\omega^2)$ involved in the dikaon DAs. Using the determined parameters of the two-kaon DAs in our previous work, we have predicted the branching ratios of $B_{(s)} \to [D^{(*)}, \bar{D}^{(*)}](R\to)KK$ decay channels. It has been shown that our predictions of the branching ratios for most of the considered decays are in good agreement with the existing data within the errors. The branching ratios of the two-body $B_{(s)} \to [D^{(*)}, \bar{D}^{(*)}]R$ can be extracted from the corresponding quasi-two-body modes by employing the narrow width approximation. Moreover, we calculated the polarization fractions of the vector-vector and vector-tensor decay modes in detail. For most of the considered channels, the transverse polarization has been found to be of similar size as the longitudinal one, which is quite different from the general expectation in the factorization assumption. More precise data from the LHCb Collaboration and the future Belle II Collaboration will test our predictions.

ACKNOWLEDGMENTS

We thank Hsiang-nan Li for valuable discussions. This work was supported by the National Natural Science Foundation of China under No. 11947013, No. 11605060, No. 11775117, and No. 11547020. Y. L. is also supported by the Natural Science Foundation of Jiangsu Province under Grant No. BK20190508 and the Research Start-up Funding of Nanjing Agricultural University. Z. R. is supported in part by the Natural Science Foundation of Hebei Province under Grant No. A2019209449.

APPENDIX: DECAY AMPLITUDES

For $B_{(s)} \to \bar{D}^{(*)}(R\to)KK$ decays (R denotes the various partial wave resonances), the expressions of the individual amplitudes $F_{e(a)}^{LL}$ and $M_{e(a)}^{LL}$ can be straightforwardly obtained by evaluating the Feyman diagrams in Fig. 1. Performing the standard PQCD calculations, one gets the following expressions of the relevant amplitudes:

(i) $B_{(s)} \to \bar{D}(f_0 \to)KK$

$$
\begin{aligned}
F_{ef_0}^{LL} = & \frac{8\pi C_F m_B^4 f_D}{\sqrt{\eta-\eta r_D^2}} \int_0^1 dx_B dz \int_0^{1/\Lambda} b db b_B db_B \phi_B(x_B, b_B) \\
& \times \Big\{ \Big[\phi_0(z) \sqrt{\eta-\eta r_D^2} (r_D^2(-2\eta(z+1)+2z+1)+(\eta-1)(z+1)) \\
& + \eta(1-r_D^2)((\phi_t(z)+\phi_s(z))(1+2z(r_D^2-1))(\eta-1)+r_D^2(\phi_t(z)-\phi_s(z))) \Big] \\
& \cdot E_e(t_a) h_a(x_B, z, b, b_B) S_t(z) \\
& + \sqrt{\eta-\eta r_D^2} \Big[\phi_0(z)(r_D^2(\eta^2-x_B)-(\eta-1)\eta) + 2\phi_s(z)\sqrt{\eta-\eta r_D^2} \\
& \cdot (\eta + r_D^2(-2\eta+x_B+1)-1) \Big] \cdot E_e(t_b) h_a(x_B, z, b_B, b) S_t(|x_B-\eta|) \Big\},
\end{aligned} \tag{A1}
$$

$$
\begin{aligned}
F_{af_0}^{LL} = & \frac{8\pi C_F m_B^4 f_B}{\sqrt{\eta-\eta r_D^2}} \int_0^1 dx_3 dz \int_0^{1/\Lambda} b db b_3 db_3 \phi_D(x_3, b_3) \\
& \times \Big\{ \Big[\phi_0(z) \sqrt{\eta-\eta r_D^2} (r_D^2(2\eta-2(\eta-1)z-1)+(\eta-1)(z-1)) - 2\eta \\
& \times r_D(r_D^2-1)^2 z(\phi_t(z)-\phi_s(z)) + 4\eta r_D(r_D^2-1)\phi_s(z) \Big] E_a(t_e) \\
& \times h_e(z, x_3, b, b_3) S_t(z) + \sqrt{\eta-\eta r_D^2} \Big[\phi_0(z)(\eta(\eta-\eta r_D^2-1)+(\eta-1)^2 \\
& \times (r_D^2-1)x_3) + 2r_D\phi_s(z)\sqrt{\eta-\eta r_D^2}(\eta-r_D^2-\eta x_3+x_3+1) \Big] \\
& \times E_a(t_f) h_f(z, x_3, b_3, b) S_t(|\eta(x_3-1)-x_3|) \Big\},
\end{aligned} \tag{A2}
$$

$$
\begin{aligned}
M_{ef_0}^{LL} = & \frac{32\pi C_F m_B^4}{\sqrt{6(\eta-\eta r_D^2)}} \int_0^1 dx_B dz dx_3 \int_0^{1/\Lambda} b_3 db_3 b_B db_B \phi_B(x_B, b_B) \phi_D(x_3, b_3) \\
& \times \Big\{ \Big[\phi_0(z)(-\eta+r_D^2+1)\sqrt{\eta-\eta r_D^2}((1-r_D^2)((x_3+x_B-1)-(x_3+z)\eta) \\
& + \eta(1-2r_D^2)) + \eta(-r_D^2+1)(\phi_t(z)((\eta-1)z(1-r_D^2)-r_D^2((1-\eta)x_3 \\
& + x_B)) + \phi_s(z)(r_D^2(x_3+2+z)-z)(\eta-1) \Big] E_n(t_c) h_c(x_B, z, x_3, b_B, b_3) \\
& - \Big[\phi_0(z)\sqrt{\eta-\eta r_D^2}(-\eta+(2\eta-1)r_D^2+1)((r_D^2-1)z+(\eta-1)x_3+x_B) \\
& + \eta(-r_D^2+1)((\phi_t(z)-\phi_s(z))r_D^2((\eta-1)x_3+x_B)+(\eta-1)z(r_D^2-1) \\
& \times (\phi_t(z)+\phi_s(z))) \Big] E_n(t_d) h_d(x_B, z, x_3, b_B, b_3) \Big\},
\end{aligned} \tag{A3}
$$

$$M^{LL}_{af_0} = \frac{32\pi C_F m_B^4}{\sqrt{6(\eta-\eta r_D^2)}}\int_0^1 dx_B dz dx_3 \int_0^{1/\Lambda} b db b_B db_B \phi_B(x_B,b_B)\phi_D(x_3,b_3)$$
$$\times\Big\{\Big[\phi_0(z)\sqrt{\eta-\eta r_D^2}(r_D^2(\eta(-\eta(x_3+z-2)+x_3+x_B)-1)+(\eta-1)(\eta(x_3$$
$$+z-1)-x_3-x_B))+\eta r_D(1-r_D^2)((\phi_t(z)-\phi_s(z))((1-\eta)(x_3-1)+x_B)$$
$$+(\phi_t(z)+\phi_s(z))z-4\phi_s(z))\Big]E_n(t_g)h_g(x_B,z,x_3,b,b_B)$$
$$-\Big[\phi_0(z)(-\eta+r_D^2-1)\sqrt{\eta-\eta r_D^2}(r_D^2(\eta(x_3+z-2)-x_3+x_B-z+1)$$
$$+(\eta-1)(1-z))+\eta r_D(1-r_D^2)((\phi_t(z)-\phi_s(z))(r_D^2-1)(z-1)+(\phi_t(z)$$
$$+\phi_s(z))(\eta-1)x_3+x_B-\eta)\Big]E_n(t_h)h_h(x_B,z,x_3,b,b_B)\Big\}. \tag{A4}$$

(ii) $B_{(s)} \to \bar{D}^*(f_0\to)KK$

$$F^{LL}_{ef_0} = -\frac{8\pi C_F m_B^4 f_{D^*}}{\sqrt{(\eta-\eta r_D^2)(1-\eta)}}\int_0^1 dx_B dz \int_0^{1/\Lambda} b db b_B db_B \phi_B(x_B,b_B)$$
$$\times\Big\{\Big[\phi_0(z)\sqrt{\eta-\eta r_D^2}(r_D^2(1-2(\eta-1)z)+(\eta-1)(z+1))$$
$$+\eta(-r_D^2+1)((\phi_s(z)+\phi_t(z))(1+2z(r_D^2-1))(\eta-1)+r_D^2(-\phi_t(z)+\phi_s(z)))\Big]$$
$$\cdot E_e(t_a)h_a(x_B,z,b,b_B)S_t(z)-\sqrt{\eta-\eta r_D^2}\Big[\phi_0(z)(-(r_D^2((\eta-2)\eta+x_B)-(\eta-1)\eta))$$
$$+2\phi_s(z)\sqrt{\eta-\eta r_D^2}(-\eta+r_D^2(x_B-1)+1)\Big]\cdot E_e(t_b)h_a(x_B,z,b_B,b)S_t(|x_B-\eta|)\Big\}, \tag{A5}$$

$$M^{LL}_{ef_0} = \frac{32\pi C_F m_B^4}{\sqrt{6(\eta-\eta r_D^2)(1-\eta)}}\int_0^1 dx_B dz dx_3 \int_0^{1/\Lambda} b_3 db_3 b_B db_B \phi_B(x_B,b_B)\phi_D(x_3,b_3)$$
$$\times\Big\{\Big[\phi_0(z)(\eta+r_D^2-1)\sqrt{\eta-\eta r_D^2}((\eta(1-x_3-z)+r_D^2\eta(x_3+z-2)$$
$$+(1-r_D^2)(x_3+x_B-1))+\eta(-r_D^2+1)(\phi_s(z)((\eta-1)z(1-r_D^2)-r_D^2((1$$
$$-\eta)x_3+x_B))+\phi_t(z)(r_D^2(x_3+2+z)-z)(\eta-1)\Big]\cdot E_n(t_c)h_c(x_B,z,x_3,b_B,b_3)$$
$$-\Big[\phi_0(z)(\eta+r_D^2-1)\sqrt{\eta-\eta r_D^2}((r_D^2-1)z+(\eta-1)x_3+x_B)$$
$$+\eta(-r_D^2+1)((\phi_t(z)-\phi_s(z))r_D^2((\eta-1)x_3+x_B)+(\phi_t(z)$$
$$+\phi_s(z))z(1-\eta)(r_D^2-1)\Big]\cdot E_n(t_d)h_d(x_B,z,x_3,b_B,b_3)\Big\}, \tag{A6}$$

$$F^{LL}_{af_0} = -\frac{8\pi C_F m_B^4 f_B}{\sqrt{1-\eta}}\int_0^1 dx_3 dz \int_0^{1/\Lambda} b db b_3 db_3 \phi_D(x_3,b_3)$$
$$\times\Big\{\Big[\phi_0(z)r_D^2(-2(\eta-1)z-1)+(\eta-1)(z-1)\Big]\cdot E_a(t_e)h_e(z,x_3,b,b_3)S_t(z)$$
$$+\Big[(r_D^2-1)\phi_0(z)\Big[(\eta-1)^2x_3-\eta(\eta+r_D^2-1)\Big]$$
$$-2(\eta-1)r_D\phi_s(z)\sqrt{\eta-\eta r_D^2}((r_D^2+(\eta-1)(1-x_3))\Big]$$
$$\cdot E_a(t_f)h_f(z,x_3,b_3,b)S_t(|\eta(x_3-1)-x_3|)\Big\}, \tag{A7}$$

$$M_{af_0}^{LL} = \frac{32\pi C_F m_B^4}{\sqrt{6(\eta-\eta r_D^2)(1-\eta)}}\int_0^1 dx_B dz dx_3 \int_0^{1/\Lambda} b db b_B db_B \phi_B(x_B,b_B)\phi_D(x_3,b_3)$$
$$\times\Big\{\Big[\phi_0(z)\sqrt{\eta-\eta r_D^2}(r_D^2((\eta-2)(x_3(1-\eta)+x_B-\eta(z-2)+1)$$
$$+(\eta-1)(\eta(x_3+z-1)-x_3-x_B))+(1-\eta)\eta r_D(1-r_D^2)((\phi_t(z)-\phi_s(z))$$
$$\times((1-x_3)(\eta-1)+x_B)-z((\phi_t(z)+\phi_s(z))\cdot E_n(t_g)h_g(x_B,z,x_3,b,b_B)$$
$$+\Big[\phi_0(z)(-\eta+r_D^2-1)\sqrt{\eta-\eta r_D^2}(r_D^2((\eta-1)(x_3-z)x_B-1)$$
$$+(\eta-1)(z-1))+(\eta-1)\eta r_D(1-r_D^2)((\phi_t(z)-\phi_s(z))(r_D^2-1)(z-1)$$
$$+((\phi_t(z)+\phi_s(z))(\eta+(1-\eta)x_3-x_B)))\Big]\cdot E_n(t_h)h_h(x_B,z,x_3,b,b_B)\Big\}, \tag{A8}$$

with the ratio $r_D = m_{D^{(*)}}/m_{B_{(s)}}$ and the color factor $C_F = 4/3$. $f_{D^{(*)}}$ (f_B) is the decay constant of the $D^{(*)}(B_{(s)})$ meson.

(iii) $B_{(s)} \to \bar{D}(\phi\to)KK$

$$F_{ef_2}^{LL} = \frac{8\pi C_F m_B^4 f_D}{\sqrt{\eta-\eta r_D^2}}\int_0^1 dx_B dz \int_0^{1/\Lambda} b db b_B db_B \phi_B(x_B,b_B)$$
$$\times\Big\{\Big[\phi_0(z)\sqrt{\eta-\eta r_D^2}(r_D^2(-2\eta(z+1)+2z+1)+(\eta-1)(z+1))$$
$$+\eta(-r_D^2+1)((\phi_t(z)+\phi_s(z))(1+2z(r_D^2-1))(\eta-1)+r_D^2(\phi_t(z)$$
$$-\phi_s(z)))\Big]\cdot E_e(t_a)h_a(x_B,z,b,b_B)S_t(z)+\sqrt{\eta-\eta r_D^2}\Big[\phi_0(z)(r_D^2(\eta^2-x_B)$$
$$-(\eta-1)\eta)+2\phi_s(z)\sqrt{\eta-\eta r_D^2}(\eta+r_D^2(-2\eta+x_B+1)-1)\Big]\cdot E_e(t_b)h_a(x_B,z,b_B,b)S_t(|x_B-\eta|)\Big\}, \tag{A9}$$

$$M_{ef_2}^{LL} = \frac{32\pi C_F m_B^4}{\sqrt{6(\eta-\eta r_D^2)}}\int_0^1 dx_B dz dx_3 \int_0^{1/\Lambda} b_3 db_3 b_B db_B \phi_B(x_B,b_B)\phi_D(x_3,b_3)$$
$$\times\Big\{\Big[\phi_0(z)(-\eta+r_D^2+1)\sqrt{\eta-\eta r_D^2}((1-r_D^2)((x_3+x_B-1)-(x_3+z)\eta)$$
$$+\eta(1-2r_D^2))+\eta(-r_D^2+1)(\phi_t(z)((\eta-1)z(1-r_D^2)-r_D^2((1-\eta)x_3$$
$$+x_B))+\phi_s(z)(r_D^2(x_3+2+z)-z)(\eta-1)\Big]\cdot E_n(t_c)h_c(x_B,z,x_3,b_B,b_3)$$
$$-\Big[\phi_0(z)\sqrt{\eta-\eta r_D^2}(-\eta+(2\eta-1)r_D^2+1)((r_D^2-1)z+(\eta-1)x_3+x_B)$$
$$+\eta(-r_D^2+1)((\phi_t(z)-\phi_s(z))r_D^2((\eta-1)x_3+x_B)+(\eta-1)z(r_D^2-1)(\phi_t(z)+\phi_s(z)))\Big]$$
$$\cdot E_n(t_d)h_d(x_B,z,x_3,b_B,b_3)\Big\}, \tag{A10}$$

$$F_{af_2}^{LL} = \frac{8\pi C_F m_B^4 f_B}{\sqrt{\eta-\eta r_D^2}}\int_0^1 dx_3 dz \int_0^{1/\Lambda} b db b_3 db_3 \phi_D(x_3,b_3)$$
$$\times\Big\{\Big[\phi_0(z)\sqrt{\eta-\eta r_D^2}(r_D^2(2\eta-2(\eta-1)z-1)+(\eta-1)(z-1))-2\eta r_D(r_D^2$$
$$-1)^2 z(\phi_t(z)-\phi_s(z))+4\eta r_D(r_D^2-1)\phi_s(z)\Big]\cdot E_a(t_e)h_e(z,x_3,b,b_3)S_t(z)$$
$$+\sqrt{\eta-\eta r_D^2}\Big[\phi_0(z)(\eta(\eta-\eta r_D^2-1)+(\eta-1)^2(r_D^2-1)x_3)+2r_D\phi_s(z)$$
$$\times(\eta-r_D^2-\eta x_3+x_3+1)\Big]\cdot E_a(t_f)h_f(z,x_3,b_3,b)S_t(|\eta(x_3-1)-x_3|)\Big\}, \tag{A11}$$

$$M^{LL}_{af_2} = \frac{32\pi C_F m_B^4}{\sqrt{6(\eta-\eta r_D^2)}}\int_0^1 dx_B dz dx_3 \int_0^{1/\Lambda} b db b_B db_B \phi_B(x_B,b_B)\phi_D(x_3,b_3)$$
$$\times\Big\{\Big[\phi_0(z)\sqrt{\eta-\eta r_D^2}(r_D^2(\eta(-\eta(x_3+z-2)+x_3+x_B)-1)+(\eta-1)(\eta(x_3$$
$$+z-1)-x_3-x_B))+\eta r_D((\phi_t(z)-\phi_s(z))((1-\eta)(x_3-1)+x_B)$$
$$+(\phi_t(z)+\phi_s(z))z-4\phi_s(z))\Big]E_n(t_g)h_g(x_B,z,x_3,b,b_B)$$
$$-\Big[\phi_0(z)(-\eta+r_D^2-1)\sqrt{\eta-\eta r_D^2}(r_D^2(\eta(x_3+z-2)-x_3+x_B-z+1)$$
$$+(\eta-1)(1-z))+\eta r_D(1-r_D^2)((\phi_t(z)-\phi_s(z))(r_D^2-1)(z-1)+(\phi_t(z)$$
$$+\phi_s(z))(\eta-1)x_3+x_B-\eta)\Big]\cdot E_n(t_h)h_h(x_B,z,x_3,b,b_B)\Big\}. \tag{A12}$$

(iv) $B_{(s)}\to\bar{D}^*(\phi\to)KK$

The formulas for the longitudinal component amplitudes A_L are as follows:

$$F^{LL}_{a\phi,L} = -\frac{8\pi C_F m_B^4 f_B}{\sqrt{1-\eta}}\int_0^1 dx_3 dz\int_0^{1/\Lambda} b db b_3 db_3 \phi_D(x_3,b_3)$$
$$\times\Big\{\Big[\phi_0(z)r_D^2(-2(\eta-1)z-1)+(\eta-1)(z-1)\Big]\cdot E_a(t_e)h_e(z,x_3,b,b_3)S_t(z)$$
$$+\Big[(r_D^2-1)\phi_0(z)((\eta-1)^2x_3-\eta(\eta+r_D^2-1))$$
$$-2(\eta-1)r_D\phi_s(z)\sqrt{\eta-\eta r_D^2}((r_D^2+(\eta-1)(1-x_3))\Big]$$
$$\cdot E_a(t_f)h_f(z,x_3,b_3,b)S_t(|\eta(x_3-1)-x_3|)\Big\}, \tag{A13}$$

$$F^{LL}_{e\phi,L} = -\frac{8\pi C_F m_B^4 f_D^*}{\sqrt{(\eta-\eta r_D^2)(1-\eta)}}\int_0^1 dx_B dz\int_0^{1/\Lambda} b db b_B db_B \phi_B(x_B,b_B)$$
$$\times\Big\{\Big[\phi_0(z)\sqrt{\eta-\eta r_D^2}(r_D^2(1-2(\eta-1)z)+(\eta-1)(z+1))$$
$$+\eta(-r_D^2+1)((\phi_s(z)+\phi_t(z))(1+2z(r_D^2-1))(\eta-1)+r_D^2(-\phi_t(z)+\phi_s(z)))\Big]$$
$$\cdot E_e(t_a)h_a(x_B,z,b,b_B)S_t(z)$$
$$-\sqrt{\eta-\eta r_D^2}\Big[\phi_0(z)(-(r_D^2((\eta-2)\eta+x_B)-(\eta-1)\eta))$$
$$+2\phi_s(z)\sqrt{\eta-\eta r_D^2}(-\eta+r_D^2(x_B-1)+1)\Big]\cdot E_e(t_b)h_a(x_B,z,b_B,b)S_t(|x_B-\eta|)\Big\}, \tag{A14}$$

$$M^{LL}_{e\phi,L} = \frac{32\pi C_F m_B^4}{\sqrt{6(\eta-\eta r_D^2)(1-\eta)}}\int_0^1 dx_B dz dx_3\int_0^{1/\Lambda} b_3 db_3 b_B db_B \phi_B(x_B,b_B)\phi_D(x_3,b_3)$$
$$\times\Big\{\Big[\phi_0(z)(\eta+r_D^2-1)\sqrt{\eta-\eta r_D^2}((\eta(1-x_3-z)+r_D^2\eta(x_3+z-2)$$
$$+(1-r_D^2)(x_3+x_B-1))+\eta(-r_D^2+1)(\phi_s(z)((\eta-1)z(1-r_D^2)-r_D^2((1$$
$$-\eta)x_3+x_B))+\phi_t(z)(r_D^2(x_3+2+z)-z)(\eta-1)\Big]\cdot E_n(t_c)h_c(x_B,z,x_3,b_B,b_3)$$
$$-\Big[\phi_0(z)(\eta+r_D^2-1)\sqrt{\eta-\eta r_D^2}((r_D^2-1)z+(\eta-1)x_3+x_B)$$
$$+\eta(-r_D^2+1)((\phi_t(z)-\phi_s(z))r_D^2((\eta-1)x_3+x_B)+(\phi_t(z)$$
$$+\phi_s(z))z(1-\eta)(r_D^2-1)\Big]\cdot E_n(t_d)h_d(x_B,z,x_3,b_B,b_3)\Big\}, \tag{A15}$$

$$M^{LL}_{a\phi,L} = \frac{32\pi C_F m_B^4}{\sqrt{6(\eta-\eta r_D^2)(1-\eta)}} \int_0^1 dx_B dz dx_3 \int_0^{1/\Lambda} b db b_B db_B \phi_B(x_B,b_B)\phi_D(x_3,b_3)$$
$$\times \Big\{ \Big[\phi_0(z)\sqrt{\eta-\eta r_D^2}\Big[r_D^2((\eta-2)(x_3(1-\eta)+x_B-\eta(z-2)+1)$$
$$+ (\eta-1)(\eta(x_3+z-1)-x_3-x_B)) + (1-\eta)\eta r_D\Big[(\phi_t(z)-\phi_s(z))\Big[(1$$
$$- x_3)(\eta-1)+x_B\Big] - z(\phi_t(z)-\phi_s(z))\Big]\Big]\Big] \cdot E_n(t_g) h_g(x_B,z,x_3,b,b_B)$$
$$+ \Big[\phi_0(z)(-\eta+r_D^2-1)\sqrt{\eta-\eta r_D^2}(r_D^2((\eta-1)(x_3-z)x_B-1)$$
$$+ (\eta-1)(z-1)) + (\eta-1)\eta r_D(1-r_D^2)((\phi_t(z)-\phi_s(z))(r_D^2-1)(z-1)$$
$$+ ((\phi_t(z)+\phi_s(z))(\eta+(1-\eta)x_3-x_B)))\Big] \cdot E_n(t_h) h_h(x_B,z,x_3,b,b_B)\Big\}. \tag{A16}$$

The transverse polarization amplitudes $A_{N,T}$ are of the following form:

$$F^{LL}_{e\phi,N} = -8\pi C_F m_B^4 f_{D^*} r_D \int_0^1 dx_B dz \int_0^{1/\Lambda} b db b_B db_B \phi_B(x_B,b_B)$$
$$\times \Big\{ \Big[\sqrt{\eta-\eta r_D^2}(r_D^2(-z)+z+2)\phi_a(z) + \phi_T(z)(\eta+(r_D^2-1)(2\eta z-1))$$
$$+ (r_D^2-1) z\sqrt{\eta-\eta r_D^2}\phi_v(z)\Big] \cdot E_e(t_a) h_a(x_B,z,b,b_B) S_t(z)$$
$$- \sqrt{\eta-\eta r_D^2}\Big[\phi_a(z)(-\eta+r_D^2+x_B-1) + \phi_v(z)(\eta+r_D^2-x_B-1)\Big]$$
$$\cdot E_e(t_b) h_a(x_B,z,b_B,b) S_t(|x_B-\eta|)\Big\}, \tag{A17}$$

$$F^{LL}_{e\phi,T} = -8\pi C_F m_B^4 f_{D^*} r_D \int_0^1 dx_B dz \int_0^{1/\Lambda} b db b_B db_B \phi_B(x_B,b_B)$$
$$\times \Big\{ \Big[(-r_D^2+1) z\sqrt{\eta-\eta r_D^2}\phi_a(z) + \phi_T(z)(\eta+(2\eta z+1)(r_D^2-1))$$
$$- \sqrt{\eta-\eta r_D^2}(r_D^2(-z)+z+2)\phi_v(z)\Big] \cdot E_e(t_a) h_a(x_B,z,b,b_B) S_t(z)$$
$$+ \sqrt{\eta-\eta r_D^2}\Big[(\phi_a(z)+\phi_v(z))(1-r_D^2) + (\phi_v(z)-\phi_a(z))(\eta-x_B)\Big]$$
$$\cdot E_e(t_b) h_a(x_B,z,b_B,b) S_t(|x_B-\eta|)\Big\}, \tag{A18}$$

$$M^{LL}_{e\phi,N} = 16\sqrt{\frac{2}{3}}\pi C_F m_B^4 r_D \int_0^1 dx_B dz dx_3 \int_0^{1/\Lambda} b_3 db_3 b_B db_B \phi_B(x_B,b_B)\phi_D(x_3,b_3)$$
$$\times \Big\{ \Big[\phi_T(z)(\eta+r_D^2\eta(x_3+z-2) + (1-r_D^2)(x_3+x_B-1) + \eta(1-x_3-z))\Big]$$
$$\cdot E_n(t_c) h_c(x_B,z,x_3,b_B,b_3)$$
$$- \Big[(2\sqrt{\eta-\eta r_D^2}\phi_a(z)((r_D^2-1)z+(\eta-1)x_3+x_B) + (r_D^2-1)\phi_T(z)((\eta$$
$$- 1)x_3+x_B-\eta z))\Big] \cdot E_n(t_d) h_d(x_B,z,x_3,b_B,b_3)\Big\}, \tag{A19}$$

$$M^{LL}_{e\phi,T} = 16\sqrt{\frac{2}{3}}\pi C_F m_B^4 r_D \int_0^1 dx_B dz dx_3 \int_0^{1/\Lambda} b_3 db_3 b_B db_B \phi_B(x_B,b_B)\phi_D(x_3,b_3)$$
$$\times \Big\{\Big[-\phi_T(z)((x_3+x_B-1)(1-r_D^2)+\eta((r_D^2-1)(x_3-z)+1))\Big]$$
$$\cdot E_n(t_c)h_c(x_B,z,x_3,b_B,b_3)$$
$$-\Big[-((r_D^2-1)\phi_T(z)(\eta(x_3+z)-x_3+x_B)+2\sqrt{\eta-\eta r_D^2}\phi_v(z)((r_D^2-1)$$
$$\times z+(\eta-1)x_3+x_B))\Big]\cdot E_n(t_d)h_d(x_B,z,x_3,b_B,b_3)\Big\}, \tag{A20}$$

$$F^{LL}_{a\phi,N} = 8\pi C_F m_B^4 f_B r_D\sqrt{\eta-\eta r_D^2}\int_0^1 dx_3 dz\int_0^{1/\Lambda} bdbb_3 db_3\phi_D(x_3,b_3)$$
$$\times\Big\{\Big[(r_D^2-1)z(\phi_a(z)-\phi_v(z))+2\phi_a(z)\Big]\cdot E_a(t_e)h_e(z,x_3,b,b_3)S_t(z)$$
$$+\Big[\phi_a(z)(r_D^2+\eta(x_3-1)-x_3-1)-\phi_v(z)(r_D^2+(1-\eta)(x_3-1))\Big]$$
$$\cdot E_a(t_f)h_f(z,x_3,b_3,b)S_t(|\eta(x_3-1)-x_3|)\Big\}, \tag{A21}$$

$$F^{LL}_{a\phi,T} = 8\pi C_F m_B^4 f_B r_D\sqrt{\eta-\eta r_D^2}\int_0^1 dx_3 dz\int_0^{1/\Lambda} bdbb_3 db_3\phi_D(x_3,b_3)$$
$$\times\Big\{\Big[(r_D^2-1)z(\phi_a(z)-\phi_v(z))-2\phi_v(z)\Big]\cdot E_a(t_e)h_e(z,x_3,b,b_3)S_t(z)$$
$$+\Big[\phi_a(z)(r_D^2+(1-\eta)(x_3-1)+\phi_v(z)(\eta-r_D^2-\eta x_3+x_3+1))\Big]$$
$$\cdot E_a(t_f)h_f(z,x_3,b_3,b)S_t(|\eta(x_3-1)-x_3|)\Big\}, \tag{A22}$$

$$M^{LL}_{a\phi,N} = 16\sqrt{\frac{2}{3}}\pi C_F m_B^4\int_0^1 dx_B dz dx_3\int_0^{1/\Lambda} bdbb_B db_B\phi_B(x_B,b_B)\phi_D(x_3,b_3)$$
$$\times\Big\{\Big[2r_D\sqrt{\eta-\eta r_D^2}\phi_a(z)+\phi_T(z)(-r_D^2((1-\eta)(x_3+z\eta)+x_B+(\eta)^2-1)$$
$$-(\eta-1)\eta z)+2r_D\sqrt{\eta-\eta r_D^2}\phi_v(z)(r_D^2(z-1)$$
$$+\eta(x_3-1)-x_3-x_B-z+1)\Big]\cdot E_n(t_g)h_g(x_B,z,x_3,b,b_B)$$
$$+\Big[(r_D^2-1)\phi_T(z)(r_D^2(\eta(x_3-1)-x_3+x_B)+\eta(1-\eta)(z-1)$$
$$+2r_D\sqrt{\eta-\eta r_D^2}\phi_v(z)((r_D^2-1)(z-1)+\eta(x_3-1)-x_3+x_B))\Big]\cdot E_n(t_h)h_h(x_B,z,x_3,b,b_B)\Big\}, \tag{A23}$$

$$M^{LL}_{a\phi,T} = 16\sqrt{\frac{2}{3}}\pi C_F m_B^4\int_0^1 dx_B dz dx_3\int_0^{1/\Lambda} bdbb_B db_B\phi_B(x_B,b_B)\phi_D(x_3,b_3)$$
$$\times\Big\{\Big[\phi_T(z)(-(r_D^2(x_B+(\eta-1)((\eta(z-1)+1-x_3))-(\eta-1)\eta z))$$
$$-2r_D\sqrt{\eta-\eta r_D^2}\phi_v(z)(\eta+r_D^2(z-1)-\eta x_3+x_3+x_B-z+3)\Big]\cdot E_n(t_g)h_g(x_B,z,x_3,b,b_B)$$
$$+\Big[(r_D^2-1)\phi_T(z)(r_D^2(\eta(x_3-1)-x_3+x_B)+(\eta-1)\eta(z-1))$$
$$+2r_D\sqrt{\eta-\eta r_D^2}\phi_v(z)(\eta+r_D^2(z-1)-\eta x_3+x_3-x_B-z+1)\Big]\cdot E_n(t_h)h_h(x_B,z,x_3,b,b_B)\Big\}. \tag{A24}$$

For the decays involving $D^{(*)}$ mesons, similarly, the corresponding decay amplitudes can be obtained by evaluating the Feyman diagrams in Fig. 2.

(i) $B_{(s)} \to D(f_0 \to)KK$

$$F_{ef_0}^{LL} = 8\pi C_F m_B^4 f_D \int_0^1 dx_B dz \int_0^{1/\Lambda} bdbb_B db_B \phi_B(x_B, b_B) \Big\{ \Big[\phi_0(z)(r_D^2(-2\eta(z+1)+2z+1)+(\eta-1)(z+1)) + \sqrt{\eta - \eta r_D^2}((\phi_t(z)+\phi_s(z))(\eta-1)(1+2z(r_D^2-1)) + r_D^2(\phi_t(z) - \phi_s(z))) \Big] \cdot E_e(t_a) h_a(x_B, z, b, b_B) S_t(z) + \Big[\phi_0(z)(r_D^2(\eta^2 - x_B) - (\eta-1)\eta) + 2\phi_s(z)\sqrt{\eta - \eta r_D^2}(\eta + r_D^2(-2\eta + x_B + 1) - 1) \Big] \cdot E_e(t_b) h_a(x_B, z, b_B, b) S_t(|x_B - \eta|) \Big\}, \tag{A25}$$

$$M_{ef_0}^{LL} = \frac{32\pi C_F m_B^4}{\sqrt{6}} \int_0^1 dx_B dz dx_3 \int_0^{1/\Lambda} b_3 db_3 b_B db_B \phi_B(x_B, b_B) \phi_D(x_3, b_3) \times \Big\{ \Big[\phi_0(z)((1-\eta)x_3(\eta(r_D^2-1)+1) - \eta(r_D^2-1)(z(-\eta + r_D^2 + 1) + x_B) - x_B) + \sqrt{\eta - \eta r_D^2}(r_D^2((\eta-1)x_3 + x_B)(\phi_s(z) + \phi_t(z)) - (\eta-1)z(r_D^2-1)(\phi_s(z) - \phi_t(z))) \Big] \cdot E_n(t_c) h_c(x_B, z, x_3, b_B, b_3) + \Big[\phi_0(z)(-\eta + (2\eta-1)r_D^2 + 1)(\eta + r_D^2(z-1) - \eta x_3 + x_3 + x_B - z - 1) + \sqrt{\eta - \eta r_D^2}(r_D^2(\phi_t(z) + \phi_s(z))((-\eta x_3 + x_3 + x_B) - 2\phi_s(z)(\eta-1)) + (r_D^2 - 1)(\eta-1)z(\phi_t(z) - \phi_s(z)) \Big] \cdot E_n(t_d) h_d(x_B, z, x_3, b_B, b_3) \Big\}, \tag{A26}$$

$$F_{aD}^{LL} = -8\pi C_F m_B^4 f_B \int_0^1 dx_3 dz \int_0^{1/\Lambda} bdbb_3 db_3 \phi_D(x_3, b_3) \Big\{ \Big[\phi_0(z)(\eta(\eta - \eta r_D^2 - 1) + (\eta-1)^2(r_D^2-1)x_3) + 2r_D\phi_s(z)\sqrt{\eta - \eta r_D^2}(-\eta + r_D^2 + (\eta-1)x_3 - 1) \Big] \cdot E_a(t_e) h_e(z, x_3, b, b_3) S_t(z) - \Big[(\eta-1)\phi_0(z)(r_D^2(\eta - 2z + 1) + z) + 2r_D\sqrt{\eta - \eta r_D^2}((\phi_t(z) + \phi_s(z))(\eta-1) + z(\phi_t(z) - \phi_s(z))) \Big] \cdot E_a(t_f) h_f(z, x_3, b_3, b) S_t(|\eta(x_3 - 1) - x_3|) \Big\}, \tag{A27}$$

$$M_{aD}^{LL} = \frac{32\pi C_F m_B^4}{\sqrt{6}} \int_0^1 dx_B dz dx_3 \int_0^{1/\Lambda} bdbb_B db_B \phi_B(x_B, b_B) \phi_D(x_3, b_3) \times \Big\{ \Big[\phi_0(z)(r_D^2((1-\eta^2)x_3 + (\eta-1)x_B + (\eta^2 + \eta - 2)z - 1) - (\eta-1)((\eta+1)(x_B + z) - \eta)) - r_D\sqrt{\eta - \eta r_D^2}((\phi_t(z) + \phi_s(z))(\eta - 1)x_3 + (\phi_t(z) - \phi_s(z))(x_B + z) - 2\phi_s(z)) \Big] \cdot E_n(t_g) h_g(x_B, z, x_3, b, b_B) - \Big[\phi_0(z)(\eta(-\eta + r_D^2 + 1)(-((r_D^2-1)z + x_B)) - (\eta-1)x_3(\eta \times (r_D^2 - 1) + 1)) - r_D\sqrt{\eta - \eta r_D^2}((\phi_t(z) + \phi_s(z))((r_D^2-1)z + x_B) + (\phi_s(z) - \phi_t(z))(\eta-1)x_3) \Big] \cdot E_n(t_h) h_h(x_B, z, x_3, b, b_B) \Big\}. \tag{A28}$$

(ii) $B_{(s)} \to D^*(f_0 \to)KK$

$$F^{LL}_{ef_0} = -\frac{8\pi C_F m_B^4 f_{D^*}}{\sqrt{(1-\eta)}} \int_0^1 dx_B dz \int_0^{1/\Lambda} b db b_B db_B \phi_B(x_B, b_B)$$
$$\times \Big\{ \Big[\phi_0(z)(r_D^2(1-2(\eta-1)z) + (\eta-1)(z+1)) + \sqrt{\eta - \eta r_D^2}$$
$$\times ((\phi_t(z) + \phi_s(z))(\eta-1)(1+2z(r_D^2-1)) + r_D^2(\phi_s(z)$$
$$- \phi_t(z))) \Big] \cdot E_e(t_a) h_a(x_B, z, b, b_B) S_t(z) - \Big[\phi_0(z)(-(r_D^2((\eta-2)\eta + x_B)$$
$$- (\eta-1)\eta)) + 2\phi_s(z)\sqrt{\eta - \eta r_D^2}(-\eta + r_D^2(x_B - 1) + 1) \Big] \cdot E_e(t_b) h_a(x_B, z, b_B, b) S_t(|x_B - \eta|) \Big\}, \quad \text{(A29)}$$

$$M^{LL}_{ef_0} = -\frac{32\pi C_F m_B^4}{\sqrt{6(1-\eta)}} \int_0^1 dx_B dz dx_3 \int_0^{1/\Lambda} b_3 db_3 b_B db_B \phi_B(x_B, b_B) \phi_D(x_3, b_3)$$
$$\times \Big\{ \Big[(r_D^2 - 1)\phi_0(z)(\eta + r_D^2 - 1)((\eta-1)x_3 + x_B - \eta z)$$
$$+ \sqrt{\eta - \eta r_D^2}((\phi_t(z) + \phi_s(z)) r_D^2((\eta-1)x_3 + x_B)$$
$$+ (\phi_t(z) - \phi_s(z))(1 - r_D^2)(\eta-1)z) \Big] \cdot E_n(t_c) h_c(x_B, z, x_3, b_B, b_3)$$
$$+ \Big[\phi_0(z)(\eta + r_D^2 - 1)(\eta + r_D^2(z-1) - (\eta-1)x_3$$
$$+ x_B - z - 1) + \sqrt{\eta - \eta r_D^2}((\phi_t(z) + \phi_s(z))((\eta-1)(1 - r_D^2)z$$
$$+ (\phi_t(z) - \phi_s(z)) r_D^2(-(\eta-1)x_3 + x_B)$$
$$+ 2r_D^2 \phi_t(z)(\eta-1)) \Big] \cdot E_n(t_d) h_d(x_B, z, x_3, b_B, b_3) \Big\}, \quad \text{(A30)}$$

$$F^{LL}_{aD} = \frac{8\pi C_F m_B^4 f_B}{\sqrt{1-\eta}} \int_0^1 dx_3 dz \int_0^{1/\Lambda} b db b_3 db_3 \phi_D(x_3, b_3)$$
$$\times \Big\{ \Big[(r_D^2 - 1)\phi_0(z)((\eta-1)^2 x_3 - \eta(\eta + r_D^2 - 1)) + 2(\eta-1) r_D \phi_s(z)$$
$$\times \sqrt{\eta - \eta r_D^2}(\eta + r_D^2 - \eta x_3 + x_3 - 1) \Big] \cdot E_a(t_e) h_e(z, x_3, b, b_3) S_t(z)$$
$$+ (1-\eta) \Big[\phi_0(z)(z - r_D^2(\eta + 2z - 1)) \Big]$$
$$\cdot E_a(t_f) h_f(z, x_3, b_3, b) S_t(|\eta(x_3 - 1) - x_3|) \Big\}, \quad \text{(A31)}$$

$$M^{LL}_{aD} = -\frac{32\pi C_F m_B^4}{\sqrt{6(1-\eta)}} \int_0^1 dx_B dz dx_3 \int_0^{1/\Lambda} b db b_B db_B \phi_B(x_B, b_B) \phi_D(x_3, b_3)$$
$$\times \Big\{ \Big[\phi_0(z)(r_D^2(\eta^2(x_3 + z) - x_3 + (\eta-1)x_B + (\eta-2)z + 1) - (\eta^2 - 1)$$
$$\times (x_B + z) + \eta(\eta-1)) + \sqrt{\eta - \eta r_D^2}(\eta-1)(-r_D)((\phi_t(z) - \phi_s(z))(1$$
$$- \eta)x_3 - 2\phi_t(z) + (\phi_t(z) + \phi_s(z))(x_B + z)) \Big] \cdot E_n(t_g) h_g(x_B, z, x_3, b, b_B)$$
$$+ \Big[\phi_0(z)(\eta + r_D^2 - 1)((\eta-1)(r_D^2 - 1)x_3 - \eta((r_D^2 - 1)z + x_B))$$
$$+ (\eta-1)(-r)\sqrt{\eta - \eta r_D^2}((\phi_t(z) - \phi_s(z))((r_D^2 - 1)z + x_B) + (\phi_t(z)$$
$$+ \phi_s(z))((\eta-1)x_3)) \Big] \cdot E_n(t_h) h_h(x_B, z, x_3, b, b_B) \Big\}. \quad \text{(A32)}$$

(iii) $B_{(s)} \to D(\phi \to)KK$

$$
\begin{aligned}
F_{e\phi}^{LL} = & \frac{8\pi C_F m_B^4 f_D}{\sqrt{\eta-\eta r_D^2}} \int_0^1 dx_B dz \int_0^{1/\Lambda} b d b b_B d b_B \phi_B(x_B, b_B) \\
& \times \Big\{ \Big[\phi_0(z) \sqrt{\eta-\eta r_D^2} (r_D^2(-2\eta(z+1)+2z+1) + (\eta-1)(z+1)) \\
& + \eta(-(r_D^2-1))((\phi_t(z)+\phi_s(z))(\eta-1)(1+2z(r_D^2-1)) \\
& + r_D^2(\phi_t(z)-\phi_s(z))) \Big] \cdot E_e(t_a) h_a(x_B, z, b, b_B) S_t(z) + \sqrt{\eta-\eta r_D^2} \\
& \times \Big[\phi_0(z)(r_D^2(\eta^2 - x_B) - (\eta-1)\eta) + 2\phi_s(z)\sqrt{\eta-\eta r_D^2}(\eta + r_D^2(-2\eta \\
& \times + x_B + 1) - 1) \Big] \cdot E_e(t_b) h_a(x_B, z, b_B, b) S_t(|x_B - \eta|) \Big\},
\end{aligned} \tag{A33}
$$

$$
\begin{aligned}
M_{e\phi}^{LL} = & \frac{32\pi C_F m_B^4}{\sqrt{6(\eta-\eta r_D^2)}} \int_0^1 dx_B dz dx_3 \int_0^{1/\Lambda} b_3 d b_3 b_B d b_B \phi_B(x_B, b_B) \phi_D(x_3, b_3) \\
& \times \Big\{ (r_D^2-1) \Big[\phi_0(z)(-(-\eta + r_D^2 + 1)) \sqrt{\eta-\eta r_D^2} ((\eta-1)x_3 + x_B - \eta z) \\
& + \eta(\phi_t(z)+\phi_s(z))(r_D^2((\eta-1)x_3 + x_B)) + (\phi_t(z) - \phi_s(z)) \\
& \times (r_D^2-1)(\eta-1)z \Big] \cdot E_n(t_c) h_c(x_B, z, x_3, b_B, b_3) \\
& - \Big[(\phi_0(z)\sqrt{\eta-\eta r_D^2}(-\eta + (2\eta-1)r_D^2 + 1)((\eta-1)(1-x_3) + r_D^2(z-1) \\
& + x_B - z) + \eta(r_D^2-1)((\phi_t(z)+\phi_s(z))(\eta-1)z(1-r_D^2) \\
& - (\phi_t(z) - \phi_s(z)) r_D^2(-\eta x_3 + x_3 + x_B) + 2r_D^2 \phi_s(z)(\eta-1)) \Big] \cdot E_n(t_d) h_d(x_B, z, x_3, b_B, b_3) \Big\},
\end{aligned} \tag{A34}
$$

$$
\begin{aligned}
F_{aD}^{LL} = & -\frac{8\pi C_F m_B^4 f_B}{\sqrt{\eta-\eta r_D^2}} \int_0^1 dx_3 dz \int_0^{1/\Lambda} b d b b_3 d b_3 \phi_D(x_3, b_3) \Big\{ \Big[\phi_0(z) \sqrt{\eta-\eta r_D^2} (\eta(\eta - \eta r_D^2 - 1) \\
& + (\eta-1)^2(r_D^2-1)x_3) - 2\eta r_D(r_D^2-1)\phi_s(z)(-\eta + r_D^2 + (\eta-1)x_3 - 1) \Big] \cdot E_a(t_e) h_e(z, x_3, b, b_3) S_t(z) \\
& - \Big[(\eta-1)\phi_0(z)\sqrt{\eta-\eta r_D^2}(r_D^2(\eta - 2z + 1) + z) \\
& + 2\eta r_D(\phi_t(z)+\phi_s(z))(\eta-1) + 2\eta r_D z(\phi_t(z) - \phi_s(z)) \Big] \\
& \cdot E_a(t_f) h_f(z, x_3, b_3, b) S_t(|\eta(x_3 - 1) - x_3|) \Big\},
\end{aligned} \tag{A35}
$$

$$
\begin{aligned}
M_{aD}^{LL} = & \frac{32\pi C_F m_B^4}{\sqrt{6(\eta-\eta r_D^2)}} \int_0^1 dx_B dz dx_3 \int_0^{1/\Lambda} b d b b_B d b_B \phi_B(x_B, b_B) \phi_D(x_3, b_3) \\
& \times \Big\{ \Big[\phi_0(z) \sqrt{\eta-\eta r_D^2} (r_D^2(\eta^2(-x_3) + x_3 + (\eta-1)x_B + (\eta^2 + \eta - 2)z - 1) \\
& - (\eta-1)(\eta(x_B + z - 1) + x_B + z)) + \eta r_D(-(\phi_t(z)+\phi_s(z))((\eta-1)x_3) \\
& + (\phi_s(z) - \phi_t(z))(x_B + z) + 2\phi_s(z)) \Big] \cdot E_n(t_g) h_g(x_B, z, x_3, b, b_B) \\
& - \Big[\phi_0(z)(-\eta + r_D^2 + 1)\sqrt{\eta-\eta r_D^2}((\eta-1)(r_D^2-1)x_3 - \eta((r_D^2-1)z + x_B)) \\
& + \eta r(r_D^2-1)((\phi_t(z)+\phi_s(z))((r_D^2-1)z + x_B) + (\eta-1)x_3 \times (\phi_s(z) - \phi_t(z))) \Big] \\
& \cdot E_n(t_h) h_h(x_B, z, x_3, b, b_B) \Big\}.
\end{aligned} \tag{A36}
$$

(iv) $B_{(s)} \to D^*(\phi \to)KK$

The formulas for the longitudinal amplitudes A_L are as follows:

$$
\begin{aligned}
F^{LL}_{ef_2,L} = & -\frac{8\pi C_F m_B^4 f_{D^*}}{\sqrt{(\eta-\eta r_D^2)(1-\eta)}}\int_0^1 dx_B dz \int_0^{1/\Lambda} b db b_B db_B \phi_B(x_B,b_B) \\
& \times \Big\{\Big[\phi_0(z)\sqrt{\eta-\eta r_D^2}(r_D^2(1-2(\eta-1)z)+(\eta-1)(z+1))+\eta(-(r_D^2-1)) \\
& \times((\phi_t(z)+\phi_s(z))(\eta-1)(1+2z(r_D^2-1)+r_D^2(\phi_s(z)-\phi_t(z)))\Big] \\
& \times E_e(t_a)h_a(x_B,z,b,b_B)S_t(z)-\sqrt{\eta-\eta r_D^2}\Big[\phi_0(z)(-(r_D^2((\eta-2)\eta+x_B) \\
& -(\eta-1)\eta))+2\phi_s(z)\sqrt{\eta-\eta r_D^2}(-\eta+r_D^2(x_B-1)+1)\Big] \\
& \times E_e(t_b)h_a(x_B,z,b_B,b)S_t(|x_B-\eta|)\Big\},
\end{aligned}
\tag{A37}
$$

$$
\begin{aligned}
F^{LL}_{aD,L} = & \frac{8\pi C_F m_B^4 f_B}{\sqrt{1-\eta}}\int_0^1 dx_3 dz \int_0^{1/\Lambda} b db b_3 db_3 \phi_D(x_3,b_3) \\
& \times\Big\{\Big[(r_D^2-1)\phi_0(z)((\eta-1)^2x_3-\eta(\eta+r_D^2-1))+2(\eta-1)r_D\phi_s(z) \\
& \times\sqrt{\eta-\eta r_D^2}(\eta+r_D^2-\eta x_3+x_3-1)\Big]E_a(t_e)h_e(z,x_3,b,b_3)S_t(z) \\
& +(1-\eta)\Big[\phi_0(z)(z-r_D^2(\eta+2z-1))\Big]E_a(t_f)h_f(z,x_3,b_3,b)S_t(|\eta(x_3-1)-x_3|)\Big\},
\end{aligned}
\tag{A38}
$$

$$
\begin{aligned}
M^{LL}_{ef_2,L} = & -\frac{32\pi C_F m_B^4}{\sqrt{6(\eta-\eta r_D^2)(1-\eta)}}\int_0^1 dx_B dz dx_3 \int_0^{1/\Lambda} b_3 db_3 b_B db_B \phi_B(x_B,b_B)\phi_D(x_3,b_3) \\
& \times\Big\{\Big[\phi_0(z)(\eta+r_D^2-1)\sqrt{\eta-\eta r_D^2}((\eta-1)x_3+x_B-\eta z) \\
& -\eta((\phi_t(z)+\phi_s(z))(r_D^2((\eta-1)x_3+x_B))+(\phi_s(z)-\phi_t(z)) \\
& \times(r_D^2-1)(\eta-1)z)\Big]E_n(t_c)h_c(x_B,z,x_3,b_B,b_3) \\
& +\Big[\phi_0(z)(\eta+r_D^2-1)\sqrt{\eta-\eta r_D^2}(\eta+r_D^2(z-1)-\eta x_3+x_3 \\
& +x_B-z-1)+\eta(r_D^2-1)((\phi_t(z)+\phi_s(z))((\eta-1)r_D^2 z \\
& -(\eta-1)z)-(\phi_t(z)-\phi_s(z))r_D^2(-\eta x_3+x_3+x_B) \\
& -2r_D^2\phi_t(z)(\eta-1))\Big]E_n(t_d)h_d(x_B,z,x_3,b_B,b_3)\Big\},
\end{aligned}
\tag{A39}
$$

$$
\begin{aligned}
M^{LL}_{aD,L} = & -\frac{32\pi C_F m_B^4}{\sqrt{6(\eta-\eta r_D^2)(1-\eta)}}\int_0^1 dx_B dz dx_3 \int_0^{1/\Lambda} b db b_B db_B \phi_B(x_B,b_B)\phi_D(x_3,b_3) \\
& \times\Big\{\Big[\phi_0(z)\sqrt{\eta-\eta r_D^2}(r_D^2(\eta^2(x_3+z)-x_3+(\eta-1)x_B+(\eta-2)z+1) \\
& -(\eta-1)(\eta(x_B+z-1)+x_B+z))+(\eta-1)\eta r_D((\phi_t(z)+\phi_s(z))(1 \\
& -\eta)x_3-2\phi_t(z)+(\phi_t(z)-\phi_s(z))(x_B+z))\Big]E_n(t_g)h_g(x_B,z,x_3,b,b_B) \\
& +\Big[\phi_0(z)(\eta+r_D^2-1)\sqrt{\eta-\eta r_D^2}((\eta-1)(r_D^2-1)x_3-\eta((r_D^2-1)z+x_B)) \\
& +(\eta-1)\eta(-r_D)(r_D^2-1)((\phi_t(z)+\phi_s(z))((r_D^2-1)z+x_B)+(\phi_t(z) \\
& -\phi_s(z))((\eta-1)x_3))\Big]E_n(t_h)h_h(x_B,z,x_3,b,b_B)\Big\}.
\end{aligned}
\tag{A40}
$$

The expressions of the transverse component $A_{N,T}$ are given by

$$F^{LL}_{ef_2,N} = -8\pi C_F m_B^4 f_{D^*} r_D \int_0^1 dx_B dz \int_0^{1/\Lambda} b db b_B db_B \phi_B(x_B, b_B) \times \Big\{ \Big[\sqrt{\eta - \eta r_D^2}(((r_D^2-1)z)(\phi_v(z) - \phi_a(z)) + 2\phi_a(z)) + \phi_T(z)(\eta + (r_D^2-1)(2\eta z - 1)) \Big] E_e(t_a) h_a(x_B, z, b, b_B) S_t(z) - \sqrt{\eta - \eta r_D^2} \Big[(\phi_a(z) - \phi_v(z))(-\eta + x_B) + (\phi_a(z) + \phi_v(z)) \times (r_D^2 - 1) \Big] E_e(t_b) h_a(x_B, z, b_B, b) S_t(|x_B - \eta|) \Big\}, \tag{A41}$$

$$F^{LL}_{ef_2,T} = -8\pi C_F m_B^4 f_{D^*} r_D \int_0^1 dx_B dz \int_0^{1/\Lambda} b db b_B db_B \phi_B(x_B, b_B) \times \Big\{ \Big[-\sqrt{\eta - \eta r_D^2}((r_D^2-1)z(\phi_a(z) - \phi_v(z)) + 2\phi_v(z)) + \phi_T(z)(\eta + (2\eta z + 1)(r_D^2 - 1)) \Big] E_e(t_a) h_a(x_B, z, b, b_B) S_t(z) - \sqrt{\eta - \eta r_D^2} \Big[(\phi_a(z) - \phi_v(z))(-\eta + x_B) - (\phi_v(z) + \phi_a(z)) \times (r_D^2 - 1) \Big] E_e(t_b) h_a(x_B, z, b_B, b) S_t(|x_B - \eta|) \Big\}, \tag{A42}$$

$$M^{LL}_{ef_2,N} = 16\sqrt{\frac{2}{3}}\pi C_F m_B^4 r_D \int_0^1 dx_B dz dx_3 \int_0^{1/\Lambda} b_3 db_3 b_B db_B \phi_B(x_B, b_B) \phi_D(x_3, b_3) \times \Big\{ \Big[(r_D^2 - 1)(-\eta x_3 + x_3 - x_B + \eta z) \Big] \phi_v(z) E_n(t_c) h_c(x_B, z, x_3, b_B, b_3) - \Big[2\sqrt{\eta - \eta r_D^2}\phi_a(z)((\eta - 1)(1 - x_3) + r_D^2(z-1) + x_B - z) - \phi_T(z)(\eta + r_D^2(\eta(x_3 + z - 2) - x_3 - x_B + 1) - \eta(x_3 + z) + x_3 + x_B - 1) \Big] E_n(t_d) h_d(x_B, z, x_3, b_B, b_3) \Big\}, \tag{A43}$$

$$M^{LL}_{ef_2,T} = 16\sqrt{\frac{2}{3}}\pi C_F m_B^4 r_D \int_0^1 dx_B dz dx_3 \int_0^{1/\Lambda} b_3 db_3 b_B db_B \phi_B(x_B, b_B) \phi_D(x_3, b_3) \times \Big\{ (r_D^2 - 1) \Big[(\eta - 1)x_3 + x_B + \eta z \Big] \phi_v(z) E_n(t_c) h_c(x_B, z, x_3, b_B, b_3) + \Big[\phi_T(z)(\eta + r_D^2(-x_3 - x_B + 1) + \eta(r_D^2 - 1)(x_3 - z) + x_3 + x_B - 1) - 2\sqrt{\eta - \eta r_D^2}\phi_v(z)((\eta - 1)(1 - x_3) + r_D^2(z-1) + x_B - z) \Big] \times E_n(t_d) h_d(x_B, z, x_3, b_B, b_3) \Big\}, \tag{A44}$$

$$F^{LL}_{aD,N} = 8\pi C_F m_B^4 f_B r_D \sqrt{\eta - \eta r_D^2} \int_0^1 dx_3 dz \int_0^{1/\Lambda} b db b_3 db_3 \phi_D(x_3, b_3) \times \Big\{ \Big[(\phi_a(z) - \phi_v(z))(\eta - \eta x_3 + x_3) + (\phi_a(z) + \phi_v(z))(-r_D^2 + 1) \Big] \times E_a(t_e) h_e(z, x_3, b, b_3) S_t(z) + \Big[(\phi_a(z) + \phi_v(z))(r_D^2(z-1) - z) + (\phi_a(z) - \phi_v(z))(\eta - 1) \Big] E_a(t_f) h_f(z, x_3, b_3, b) S_t(|\eta(x_3 - 1) - x_3|) \Big\}, \tag{A45}$$

$$F_{aD,T}^{LL} = 8\pi C_F m_B^4 f_B r_D \sqrt{\eta - \eta r_D^2} \int_0^1 dx_3 dz \int_0^{1/\Lambda} b db b_3 db_3 \phi_D(x_3, b_3)$$
$$\times \Big\{ \Big[(\phi_a(z) - \phi_v(z))(-\eta + \eta x_3 - x_3)) + (\phi_a(z) + \phi_v(z))(-r_D^2 + 1) \Big]$$
$$\times E_a(t_e) h_e(z, x_3, b, b_3) S_t(z) + \Big[(\phi_a(z) + \phi_v(z))(r_D^2(z-1) - z) + (\phi_a(z)$$
$$- \phi_v(z))(-\eta + 1) \Big] E_a(t_f) h_f(z, x_3, b_3, b) S_t(|\eta(x_3 - 1) - x_3|) \Big\}, \tag{A46}$$

$$M_{aD,N}^{LL} = 16\sqrt{\frac{2}{3}}\pi C_F m_B^4 \int_0^1 dx_B dz dx_3 \int_0^{1/\Lambda} b db b_B db_B \phi_B(x_B, b_B) \phi_D(x_3, b_3)$$
$$\times \Big\{ \Big[2 r_D \phi_a(z) \sqrt{\eta - \eta r_D^2} + \phi_T(z)(r_D^2(-\eta(x_3 + z) + x_3 + \eta^2 z - 1)$$
$$- (\eta - 1)\eta(x_B + z - 1)) \Big] E_n(t_g) h_g(x_B, z, x_3, b, b_B)$$
$$+ \Big[\phi_T(z)(-1 + \eta)(-(r_D^2 - 1) r_D^2 x_3 - \eta((r_D^2 - 1)z + x_B)) \Big]$$
$$\times E_n(t_h) h_h(x_B, z, x_3, b, b_B) \Big\}, \tag{A47}$$

$$M_{aD,T}^{LL} = 16\sqrt{\frac{2}{3}}\pi C_F m_B^4 \int_0^1 dx_B dz dx_3 \int_0^{1/\Lambda} b db b_B db_B \phi_B(x_B, b_B) \phi_D(x_3, b_3)$$
$$\times \Big\{ \Big[\phi_T(z)(r_D^2(-(\eta - 1)(x_3 + \eta z) - 1) + (\eta - 1)\eta(x_B + z - 1))$$
$$+ 2 r_D \sqrt{\eta - \eta r_D^2} \phi_v(z) \Big] E_n(t_g) h_g(x_B, z, x_3, b, b_B) + \Big[\phi_T(z)(-1 + \eta)$$
$$\times (r_D^2(x_3 + \eta z) - \eta(z - x_B)) \Big] E_n(t_h) h_h(x_B, z, x_3, b, b_B) \Big\}. \tag{A48}$$

For D-wave decay amplitude $\mathcal{A}_D$, its factorization formula can be related to $\mathcal{A}_P$ by making the following replacement:

$$\mathcal{A}_D^0 = \sqrt{\frac{2}{3}} \mathcal{A}_P^0 |_{\phi_P^{0,s,t} \to \phi_D^{0,s,t}}, \qquad \mathcal{A}_D^{\parallel,\perp} = \sqrt{\frac{1}{2}} \mathcal{A}_P^{\parallel,\perp} |_{\phi_P^{T,v,a} \to \phi_D^{T,v,a}}. \tag{A49}$$

The evolution factors $E_i(t)(i = e, a, n)$ in the above equations are written in the form

$$E_e(t) = \alpha_s(t) \exp\Big[-S_B(t) - S_R(t) \Big], \tag{A50}$$

$$E_a(t) = \alpha_s(t) \exp\Big[-S_D(t) - S_R(t) \Big], \tag{A51}$$

$$E_n(t) = \alpha_s(t) \exp\Big[-S_B(t) - S_R(t) - S_D(t) \Big], \tag{A52}$$

where Sudakov exponents $S_{B,D,R}$ are defined as

$$S_B = s\left(x_B \frac{m_B}{\sqrt{2}}, b_B \right) + \frac{5}{3} \int_{1/b_B}^{t} \frac{d\bar{\mu}}{\bar{\mu}} \gamma_q(\alpha_s(\bar{\mu})), \tag{A53}$$

$$S_R = s\left(z(1 - r_D^2) \frac{m_B}{\sqrt{2}}, b \right) + s\left((1 - z)(1 - r_D^2) \frac{m_B}{\sqrt{2}}, b \right) + 2 \int_{1/b}^{t} \frac{d\bar{\mu}}{\bar{\mu}} \gamma_q(\alpha_s(\bar{\mu})), \tag{A54}$$

$$S_D = s\left(x_3(1-\eta)\frac{m_B}{\sqrt{2}}, b_3\right) + 2\int_{1/b_3}^{t}\frac{d\bar{\mu}}{\bar{\mu}}\gamma_q(\alpha_s(\bar{\mu})), \tag{A55}$$

with the quark anomalous dimension $\gamma_q = -\alpha_s/\pi$. The explicit expressions of the functions $(s(x_B m_B/\sqrt{2}, b_B)\cdots)$ can be found in the Appendix of Ref. [23].

The threshold resummation factor $S_t(x)$ is of the form

$$S_t(x) = \frac{2^{1+2c}\Gamma(3/2+c)}{\sqrt{\pi}\Gamma(1+c)}\Big[x(1-x)\Big]^c. \tag{A56}$$

The value of c is 0.3 in numerical calculations.

The hard functions $h_i(i = a-h)$ in the above amplitudes can be derived from the Fourier transform of a hard kernel:

$$h_i(x1, x2(, x3), b_1, b_2) = h_1(\beta, b_2)\times h_2(\alpha, b_1, b_2), \tag{A57}$$

$$h_1(\beta, b_2) = \begin{cases} K_0(\sqrt{\beta}b_2), & \beta > 0 \\ K_0(i\sqrt{-\beta}b_2), & \beta < 0 \end{cases} \tag{A58}$$

$$h_2(\alpha, b_1, b_2) = \begin{cases} \theta(b_2-b_1)I_0(\sqrt{\alpha}b_1)K_0(\sqrt{\alpha}b_2) + (b_1 \leftrightarrow b_2), & \alpha > 0 \\ \theta(b_2-b_1)I_0(\sqrt{-\alpha}b_1)K_0(i\sqrt{-\alpha}b_2) + (b_1 \leftrightarrow b_2), & \alpha < 0 \end{cases} \tag{A59}$$

where $K_0(ix) = \frac{\pi}{2}(-N_0(x) + iJ_0(x))$. α and β are the factors $a_{1i} - h_{1i}$ and $e_{2i} - h_{2i}$ $(i = 1, 2)$ given in the following paragraph.

The hard scales t_i that appeared in the above equations are chosen as the maximum of the virtuality of the internal momentum transition in the hard amplitudes. For $B_{(s)} \to \bar{D}^{(*)}(R\to)KK$ decays, we have

$$\begin{aligned}
t_{a_1} &= \max\left\{m_B\sqrt{|a_{11}|}, m_B\sqrt{|a_{12}|}, 1/b, 1/b_B\right\}, \qquad t_{b_1} = \max\left\{m_B\sqrt{|b_{11}|}, m_B\sqrt{|b_{12}|}, 1/b, 1/b_B\right\}, \\
t_{c_1} &= \max\left\{m_B\sqrt{|c_{11}|}, m_B\sqrt{|c_{12}|}, 1/b_3, 1/b_B\right\}, \qquad t_{d_1} = \max\left\{m_B\sqrt{|d_{11}|}, m_B\sqrt{|d_{12}|}, 1/b_3, 1/b_B\right\}, \\
t_{e_1} &= \max\left\{m_B\sqrt{|e_{11}|}, m_B\sqrt{|e_{12}|}, 1/b, 1/b_3\right\}, \qquad t_{f_1} = \max\left\{m_B\sqrt{|f_{11}|}, m_B\sqrt{|f_{12}|}, 1/b, 1/b_3\right\}, \\
t_{g_1} &= \max\left\{m_B\sqrt{|g_{11}|}, m_B\sqrt{|g_{12}|}, 1/b, 1/b_B\right\}, \qquad t_{h_1} = \max\left\{m_B\sqrt{|h_{11}|}, m_B\sqrt{|h_{12}|}, 1/b, 1/b_B\right\},
\end{aligned} \tag{A60}$$

with the factors

$$\begin{aligned}
&a_{11} = (1-r_D^2)z, \qquad a_{12} = (1-r_D^2)x_B z, \qquad b_{11} = (1-r_D^2)(x_B-\eta), \qquad b_{12} = a_{12}, \\
&c_{11} = a_{12}, \qquad c_{12} = [(1-r_D^2)z + r_D^2][x_B - (1-\eta)(1-x_3)], \\
&d_{11} = a_{12}, \qquad d_{12} = (1-r_D^2)z[x_B - (1-\eta)x_3], \\
&e_{11} = z(1-r_D^2) - 1, \qquad e_{12} = (z-1)(r_D^2-1)[(\eta-1)x_3 - \eta], \\
&f_{11} = (1-r_D^2)[(\eta-1)x_3 - \eta], \qquad f_{12} = e_{12}, \\
&g_{11} = e_{12}, \qquad g_{12} = 1 - [(1-z)r_D^2 + z][(1-\eta)(1-x_3) - x_B], \\
&h_{11} = e_{12}, \qquad h_{12} = (1-z)(1-r_D^2)[(\eta-1)x_3 - \eta + x_B].
\end{aligned} \tag{A61}$$

While for $B_{(s)} \to D^{(*)}(R \to)KK$ decays, similarly, we have

$$t_{a_1} = \max\left\{m_B\sqrt{|a_{11}|}, m_B\sqrt{|a_{12}|}, 1/b, 1/b\right\}, \qquad t_{b_1} = \max\left\{m_B\sqrt{|b_{11}|}, m_B\sqrt{|b_{12}|}, 1/b, 1/b_B\right\},$$
$$t_{c_1} = \max\left\{m_B\sqrt{|c_{11}|}, m_B\sqrt{|c_{12}|}, 1/b_3, 1/b_B\right\}, \qquad t_{d_1} = \max\left\{m_B\sqrt{|d_{11}|}, m_B\sqrt{|d_{12}|}, 1/b_3, 1/b_B\right\},$$
$$t_{e_2} = \max\left\{m_B\sqrt{|e_{21}|}, m_B\sqrt{|e_{22}|}, 1/b, 1/b_3\right\}, \qquad t_{f_2} = \max\left\{m_B\sqrt{|f_{21}|}, m_B\sqrt{|f_{22}|}, 1/b, 1/b_3\right\},$$
$$t_{g_2} = \max\left\{m_B\sqrt{|g_{21}|}, m_B\sqrt{|g_{22}|}, 1/b, 1/b_B\right\}, \qquad t_{h_2} = \max\left\{m_B\sqrt{|h_{21}|}, m_B\sqrt{|h_{22}|}, 1/b, 1/b_B\right\}, \tag{A62}$$

with the factors

$$a_{11} = (1-r_D^2)z, \qquad a_{12} = (1-r_D^2)x_B z, \qquad b_{11} = (1-r_D^2)(x_B-\eta), \qquad b_{12} = a_{12},$$
$$c_{11} = a_{12}, \qquad c_{12} = (1-r_D^2)z(x_B-(1-\eta)x_3),$$
$$d_{11} = a_{12}, \qquad d_{12} = ((z-1)r_D^2 - z)[(1-\eta)(1-x_3) - x_B],$$
$$e_{21} = (1-r_D^2)[(x_3-1)\eta - x_3], \qquad e_{22} = (1-\eta)(r_D^2-1)x_3 z, \qquad f_{21} = (\eta-1)[z + r_D^2(1-z)],$$
$$f_{22} = e_{12}, \qquad g_{21} = e_{22}, \qquad g_{22} = [1-(1-\eta)x_3][(1-r_D^2)z + x_B] + (1-\eta)x_3,$$
$$h_{21} = e_{22}, \qquad h_{22} = (1-\eta)x_3[x_B - (1-r_D^2)z]. \tag{A63}$$

[1] M. Gronau and D. London, How to determine all the angles of the unitarity triangle from $B_d^0 \to DK_S$ and $B_s^0 \to D\phi$, Phys. Lett. B **253**, 483 (1991).

[2] M. Gronau, Y. Grossman, N. Shuhmaher, A. Soffer, and J. Zupan, Using untagged $B^0 \to DK_S$ to determine γ, Phys. Rev. D **69**, 113003 (2004).

[3] M. Gronau, Y. Grossman, Z. Surujon, and J. Zupan, Enhanced effects on extracting γ from untagged B^0 and B_s decays, Phys. Lett. B **649**, 61 (2007).

[4] B. Aubert *et al.* (*BABAR* Collaboration), Search for rare quark-annihilation decays, $B^- \to D_s^{(*)-}\phi$, Phys. Rev. D **73**, 011103 (2006).

[5] B. Aubert *et al.* (*BABAR* Collaboration), Search for $B^0 \to \phi(K^+\pi^-)$ decays with large $K^+\pi^-$ invariant mass, Phys. Rev. D **76**, 051103 (2007).

[6] B. Aubert *et al.* (*BABAR* Collaboration), Observation of Tree-Level B Decays with $s\bar{s}$ Production from Gluon Radiation, Phys. Rev. Lett. **100**, 171803 (2008).

[7] J. P. Lees *et al.* (*BABAR* Collaboration), Amplitude analysis and measurement of the time-dependent CP asymmetry of $B^0 \to K_S^0 K_S^0 K_S^0$ decays, Phys. Rev. D **85**, 054023 (2012).

[8] J. P. Lees *et al.* (*BABAR* Collaboration), Study of CP violation in Dalitz-plot analyses of $B^0 \to K^+K^-K_S^0$, $B^+ \to K^+K^-K^+$, and $B^+ \to K_S^0 K_S^0 K^+$, Phys. Rev. D **85**, 112010 (2012).

[9] A. Drutskoy *et al.* (Belle Collaboration), Observation of $B \to D^{(*)}K^-K^{0(*)}$ decays, Phys. Lett. B **542**, 171 (2002).

[10] A. Kuzmin *et al.* (Belle Collaboration), Study of $\bar{B}^0 \to D^0\pi^+\pi^-$ decays, Phys. Rev. D **76**, 012006 (2007).

[11] J. Wiechczynski *et al.* (Belle Collaboration), Measurement of $B^0 \to D_s^- K_S^0 \pi^+$ and $B^+ \to D_s^- K^+K^+$ branching fractions, Phys. Rev. D **91**, 032008 (2015).

[12] R. Aaij *et al.* (LHCb Collaboration), Observation of $B^0 \to \bar{D}^0 K^+K^-$ and Evidence for $B_s^0 \to \bar{D}^0 K^+K^-$, Phys. Rev. Lett. **109**, 131801 (2012).

[13] R. Aaij *et al.* (LHCb Collaboration), First evidence for the annihilation decay mode $B^+ \to D_s^+\phi$, J. High Energy Phys. 02 (2013) 043.

[14] R. Aaij *et al.* (LHCb Collaboration), Observation of the decay $B_s^0 \to \bar{D}^0\phi$, Phys. Lett. B **727**, 403 (2013).

[15] R. Aaij *et al.* (LHCb Collaboration), Search for the decay $B_s^0 \to \bar{D}^0 f_0(980)$, J. High Energy Phys. 08 (2015) 005.

[16] R. Aaij *et al.* (LHCb Collaboration), Dalitz plot analysis of $B^0 \to \bar{D}^0\pi^+\pi^-$ decays, Phys. Rev. D **92**, 032002 (2015).

[17] R. Aaij *et al.* (LHCb Collaboration), First observation of $B^+ \to D_s^+ K^+K^-$ decays and a search for $B^+ \to D_s^+\phi$ decays, J. High Energy Phys. 01 (2018) 131.

[18] R. Aaij *et al.* (LHCb Collaboration), Observation of $B_s^0 \to \bar{D}^{*0}\phi$ and search for $B^0 \to \bar{D}^0\phi$ decays, Phys. Rev. D **98**, 071103 (2018).

[19] R. Aaij *et al.* (LHCb Collaboration), Observation of the decay $B_s^0 \to \bar{D}^0 K^+K^-$, Phys. Rev. D **98**, 072006 (2018).

[20] T. Kurimoto, H. N. Li, and A. I. Sanda, $B \to D^{(*)}$ form factors in perturbative QCD, Phys. Rev. D **67**, 054028 (2003).

[21] Y. Y. Keum, T. Kurimoto, H. N. Li, C. D. Lü, and A. I. Sanda, Nonfactorizable contributions to $B \to D^{(*)}M$ decays, Phys. Rev. D **69**, 094018 (2004).

[22] Y. Li and C. D. Lü, Calculation of rare decay $B^+ \to D_s^+ \bar{K}^{*0}$ in perturbative QCD approach, High Energy Phys. Nucl. Phys. **27**, 1062 (2003), arXiv:hep-ph/0305278.

[23] R. H. Li, C. D. Lü, and H. Zou, $B(B_s) \to D_{(s)}P, D_{(s)}V, D^*_{(s)}P$, and $D^*_{(s)}V$ decays in the perturbative QCD approach, Phys. Rev. D **78**, 014018 (2008).

[24] H. Zou, R. H. Li, X. X. Wang, and C. D. Lü, The CKM suppressed $B(B_s) \to \bar{D}_{(s)}P, \bar{D}_{(s)}V, \bar{D}^*_{(s)}P, \bar{D}^*_{(s)}V$ decays in the perturbative QCD approach, J. Phys. G **37**, 015002 (2010).

[25] Z. T. Zou, X. Yu, and C. D. Lü, $B(B_s) \to D_{(s)}(\bar{D}_{(s)})T$ and $D^*_{(s)}(\bar{D}^*_{(s)})T$ decays in perturbative QCD approach, Phys. Rev. D **86**, 094001 (2012).

[26] Z. T. Zou, Y. Li, and X. Liu, Cabibbo-Kobayashi-Maskawa-favored B decays to a scalar meson and a D meson, Eur. Phys. J. C **77**, 870 (2017).

[27] S. Mantry, D. Pirjol, and I. W. Stewart, Strong phases and factorization for color suppressed decays, Phys. Rev. D **68**, 114009 (2003).

[28] F. U. Bernlochner, Z. Ligeti, M. Papucci, and D. J. Robinson, Combined analysis of semileptonic B decays to D and D^*: $R(D^{(*)})$, $|V_{ub}|$, and new physics, Phys. Rev. D **95**, 115008 (2017).

[29] S. Jaiswal, S. Nandi, and S. K. Patra, Extraction of $|V_{cb}|$ from $B \to D^{(*)}l\nu_l$ and the Standard Model predictions of $R(D^{(*)})$, J. High Energy Phys. 12 (2017) 060.

[30] S. Faller, A. Khodjamirian, C. Klein, and T. Mannel, $B \to D^{(*)}$ form factors from QCD light-cone sum rules, Eur. Phys. J. C **60**, 603 (2009).

[31] Y. M. Wang, Y. B. Wei, Y. L. Shen, and C. D. Lü, Perturbative corrections to $B \to D$ form factors in QCD, J. High Energy Phys. 06 (2017) 062.

[32] Y. Zhang, T. Zhong, X. G. Wu, K. Li, H. B. Fu, and T. Huang, Uncertainties of the $B \to D$ transition form factor from the D-meson leading-twist distribution amplitude, Eur. Phys. J. C **78**, 76 (2018).

[33] T. Bhattacharya *et al.* (LANL/SWME Collaboration), Update on $B \to D^* l\nu$ form factor at zero-recoil using the Oktay-Kronfeld action, Proc. Sci., LATTICE2018 (**2018**) 283 [arXiv:1812.07675].

[34] J. A. Bailey *et al.* (LANL/SWME Collaboration), Calculation of $B \to D^* l\nu$ form factor at zero recoil using the Oktay-Kronfeld action, EPJ Web Conf. **175**, 13012 (2018).

[35] T. Kaneko *et al.* (JLQCD Collaboration), $B \to D^{(*)}l\nu$ form factors from $N_f = 2 + 1$ QCD with Möbius domain-wall quarks, Proc. Sci., LATTICE2018 (**2018**) 311 [arXiv:1811.00794].

[36] I. Bediaga, T. Frederico, and O. Lourenço, CP violation and CPT invariance in $B^{\pm}$ decays with final state interactions, Phys. Rev. D **89**, 094013 (2014).

[37] I. Bediaga and P. C. Magalhães, Final state interaction on $B^+ \to \pi^-\pi^+\pi^+$, arXiv:1512.09284.

[38] X. W. Kang, B. Kubis, C. Hanhart, and U. G. Meißner, B_{l4} decays and the extraction of $|V_{ub}|$, Phys. Rev. D **89**, 053015 (2014).

[39] R. H. Dalitz, On the analysis of τ-meson data and the nature of the τ-meson, Philos. Mag. Ser. 5 **44**, 1068 (1953).

[40] R. H. Dalitz, Decay of τ mesons of known charge, Phys. Rev. **94**, 1046 (1954).

[41] J. Virto, Charmless non-leptonic multi-body B decays, Proc. Sci., FPCP2016 (**2017**) 007 [arXiv:1609.07430].

[42] S. Kränkl, T. Mannel, and J. Virto, Three-body nonleptonic B decays and QCD factorization, Nucl. Phys. **B899**, 247 (2015).

[43] D. Müller, D. Robaschik, B. Geyer, F.-M. Dittes, and J. Hořejši, Wave functions, evolution equations and evolution kernels from light ray operators of QCD, Fortschr. Phys. **42**, 101 (1994).

[44] M. Diehl, T. Gousset, B. Pire, and O. Teryaev, Probing Partonic Structure in $\gamma^*\gamma \to \pi\pi$ near Threshold, Phys. Rev. Lett. **81**, 1782 (1998).

[45] M. Diehl, T. Gousset, and B. Pire, Exclusive production of pion pairs in $\gamma^*\gamma$ collisions at large Q^2, Phys. Rev. D **62**, 073014 (2000).

[46] Ph. Hägler, B. Pire, L. Szymanowski, and O. V. Teryaev, Pomeron-odderon interference effects in electroproduction of two pions, Eur. Phys. J. C **26**, 261 (2002).

[47] M. V. Polyakov, Hard exclusive electroproduction of two pions and their resonances, Nucl. Phys. **B555**, 231 (1999).

[48] A. G. Grozin, On wave functions of mesonic pairs and mesonic resonances, Sov. J. Nucl. Phys. **38**, 289 (1983).

[49] A. G. Grozin, One-and two-particle wave functions of multihadron systems, Theor. Math. Phys. **69**, 1109 (1986).

[50] C. H. Chen and H. N. Li, Three body nonleptonic B decays in perturbative QCD, Phys. Lett. B **561**, 258 (2003).

[51] W. F. Wang and H. N. Li, Quasi-two-body decays $B \to K\rho \to K\pi\pi$ in perturbative QCD approach, Phys. Lett. B **763**, 29 (2016).

[52] Y. Li, A. J. Ma, W. F. Wang, and Z. J. Xiao, The S-wave resonance contributions to the three-body decays $B^0_{(s)} \to \eta_c f_0(X) \to \eta_c \pi^+\pi^-$ in perturbative QCD approach, Eur. Phys. J. C **76**, 675 (2016).

[53] A. J. Ma, Y. Li, W. F. Wang, and Z. J. Xiao, S-wave resonance contributions to the $B^0_{(s)} \to \eta_c(2S)\pi^+\pi^-$ in the perturbative QCD factorization approach, Chin. Phys. C **41**, 083105 (2017).

[54] Z. Rui, Y. Li, and W. F. Wang, The S-wave resonance contributions in the B^0_s decays into $\psi(2S, 3S)$ plus pion pair, Eur. Phys. J. C **77**, 199 (2017).

[55] Z. Rui and W. F. Wang, The S-wave $K\pi$ contributions to the hadronic charmonium B decays in the perturbative QCD approach, Phys. Rev. D **97**, 033006 (2018).

[56] Y. Li, A. J. Ma, W. F. Wang, and Z. J. Xiao, Quasi-two-body decays $B_{(s)} \to P\rho \to P\pi\pi$ in the perturbative QCD approach, Phys. Rev. D **95**, 056008 (2017).

[57] A. J. Ma, Y. Li, W. F. Wang, and Z. J. Xiao, Quasi-two-body decays $B_{(s)} \to D(\rho(1450), \rho(1700)) \to D\pi\pi$ in the perturbative QCD factorization approach, Phys. Rev. D **96**, 093011 (2017).

[58] Y. Li, W. F. Wang, A. J. Ma, and Z. J. Xiao, Quasi-two-body decays $B_{(s)} \to K^*(892)h \to K\pi h$ in perturbative QCD approach, Eur. Phys. J. C **79**, 37 (2019).

[59] A. J. Ma, W. F. Wang, Y. Li, and Z. J. Xiao, Quasi-two-body decays $B \to DK^*(892) \to DK\pi$ in the perturbative QCD approach, Eur. Phys. J. C **79**, 539 (2019).

[60] N. Wang, Q. Chang, Y. L. Yang, and J. F. Sun, Study of the $B_s \to \phi f_0(980) \to \phi\pi^+\pi^-$ decay with perturbative QCD approach, J. Phys. G **46**, 095001 (2019).

[61] Z. Rui, Y. Li, and H. Li, Studies of the resonance components in the B_s decays into charmonia plus kaon pair, Eur. Phys. J. C **79**, 792 (2019).

[62] Y. Li, Z. Rui, and Z. J. Xiao, P-wave contributions to $B_{(s)} \to \psi K\pi$ decays in perturbative QCD approach, Chin. Phys. C **44**, 073102 (2020).

[63] W. F. Wang, J. Chai, and A. J. Ma, Contributions of $K_0^*(1430)$ and $K_0^*(1950)$ in the three-body decays $B \to K\pi h$, J. High Energy Phys. 03 (2020) 162.

[64] W. F. Wang, Will the subprocesses $\rho(770, 1450)^0 \to K^+K^-$ contribute large branching fractions for $B^\pm \to \pi^\pm K^+K^-$ decays?, Phys. Rev. D **101**, 111901 (2020).

[65] Z. T. Zou, Y. Li, Q. X. Li, and X. Liu, Resonant contributions to three-body $B \to KKK$ decays in perturbative QCD approach, Eur. Phys. J. C **80**, 394 (2020).

[66] Z. T. Zou, Y. Li, and X. Liu, Branching fractions and CP asymmetries of the quasi-two-body decays in $B_s \to K^0(\bar{K}^0)K^\pm\pi^\mp$ within PQCD approach, Eur. Phys. J. C **80**, 517 (2020).

[67] Y. Xing and Z. P. Xing, S-wave contributions to $\bar{B}_s^0 \to (D^0, \bar{D}^0)\pi^+\pi^-$ in the perturbative QCD framework, Chin. Phys. C **43**, 073103 (2019).

[68] Z. Rui, Y. Q. Li, and J. Zhang, Isovector scalar $a_0(980)$ and $a_0(1450)$ resonances in the $B \to \psi(K\bar{K}, \pi\eta)$ decays, Phys. Rev. D **99**, 093007 (2019).

[69] M. Beneke, G. Buchalla, M. Neubert, and C. T. Sachrajda, QCD Factorization for $B \to \pi\pi$ Decays: Strong Phases and CP Violation in the Heavy Quark Limit, Phys. Rev. Lett. **83**, 1914 (1999).

[70] M. Beneke, G. Buchalla, M. Neubert, and C. T. Sachrajda, QCD factorization for exclusive, nonleptonic B meson decays: General arguments and the case of heavy-light final states, Nucl. Phys. **B591**, 313 (2000).

[71] M. Beneke, G. Buchalla, M. Neubert, and C. T. Sachrajda, QCD factorization in $B \to \pi K, \pi\pi$ decays and extraction of Wolfenstein parameters, Nucl. Phys. **B606**, 245 (2001).

[72] M. Beneke and M. Neubert, QCD factorization for $B \to PP$ and $B \to PV$ decays, Nucl. Phys. **B675**, 333 (2003).

[73] A. Furman, R. Kamiński, L. Leśniak, and B. Loiseau, Long-distance effects and final state interactions in $B \to \pi\pi K$ and $B \to K\bar{K}K$ decays, Phys. Lett. B **622**, 207 (2005).

[74] B. El-Bennich, A. Furman, R. Kamiński, L. Leśniak, and B. Loiseau, Interference between $f_0(980)$ and $\rho(770)^0$ resonances in $B \to \pi^+\pi^-K$ decays, Phys. Rev. D **74**, 114009 (2006).

[75] B. El-Bennich, A. Furman, R. Kamiński, L. Leśniak, B. Loiseau, and B. Moussallam, CP violation and kaon-pion interactions in $B \to K\pi^+\pi^-$ decays, Phys. Rev. D **79**, 094005 (2009).

[76] J. P. Dedonder, A. Furman, R. Kamiński, L. Leśniak, and B. Loiseau, S-, P- and D-wave $\pi\pi$ final state interactions and CP violation in $B^\pm \to \pi^\pm\pi^\mp\pi^\pm$ decays, Acta Phys. Pol. B **42**, 2013 (2011).

[77] H. Y. Cheng, C. K. Chua, and A. Soni, Charmless three-body decays of B mesons, Phys. Rev. D **76**, 094006 (2007).

[78] H. Y. Cheng and C. K. Chua, Branching fractions and direct CP violation in charmless three-body decays of B mesons, Phys. Rev. D **88**, 114014 (2013).

[79] H. Y. Cheng, C. K. Chua, and Z. Q. Zhang, Direct CP violation in charmless three-body decays of B mesons, Phys. Rev. D **94**, 094015 (2016).

[80] Y. Li, Comprehensive study of $\bar{B}^0 \to K^0(\bar{K}^0)K^\mp\pi^\pm$ decays in the factorization approach, Phys. Rev. D **89**, 094007 (2014).

[81] Z. H. Zhang, X. H. Guo, and Y. D. Yang, CP violation in $B^\pm \to \pi^\pm\pi^+\pi^-$ in the region with low invariant mass of one $\pi^+\pi^-$ pair, Phys. Rev. D **87**, 076007 (2013).

[82] R. Klein, T. Mannel, J. Virtob, and K. Keri Vos, CP violation in multibody B decays from QCD factorization, J. High Energy Phys. 10 (2017) 117.

[83] H. Y. Cheng, CP violation in $B^\pm \to \rho^0\pi^\pm$ and $B^\pm \to \sigma\pi^\pm$ decays, arXiv:2005.06080.

[84] J. J. Qi, Z. Y. Wang, X. H. Guo, Z. H. Zhang, and C. Wang, Study of CP violation in $B^- \to K^-\pi^+\pi^-$ and $B^- \to K^-\sigma(600)$ decays in the QCD factorization approach, Phys. Rev. D **99**, 076010 (2019).

[85] M. Gronau and J. L. Rosner, Symmetry relations in charmless $B \to PPP$ decays, Phys. Rev. D **72**, 094031 (2005).

[86] M. Gronau, U-spin breaking in CP asymmetries in B decays, Phys. Lett. B **727**, 136 (2013).

[87] G. Engelhard, Y. Nir, and G. Raz, $SU(3)$ Relations and the CP asymmetry in $B \to K_S K_S K_S$, Phys. Rev. D **72**, 075013 (2005).

[88] M. Imbeault and D. London, $SU(3)$ breaking in charmless B decays, Phys. Rev. D **84**, 056002 (2011).

[89] D. Xu, G. N. Li, and X. G. He, U-spin analysis of CP violation in B^- decays into three charged light pseudoscalar mesons, Phys. Lett. B **728**, 579 (2014).

[90] X. G. He, G. N. Li, and D. Xu, $SU(3)$ and isospin breaking effects on $B \to PPP$ amplitudes, Phys. Rev. D **91**, 014029 (2015).

[91] H. N. Li and Y. M. Wang, Non-dipolar Wilson links for transverse-momentum-dependent wave functions, J. High Energy Phys. 06 (2015) 013.

[92] H. N. Li, Y. L. Shen, and Y. M. Wang, Resummation of rapidity logarithms in B meson wave functions, J. High Energy Phys. 02 (2013) 008.

[93] G. Buchalla, A. J. Buras, and M. E. Lautenbacher, Weak decays beyond leading logarithms, Rev. Mod. Phys. **68**, 1125 (1996).

[94] T. Kurimoto, H. N. Li, and A. I. Sanda, Leading-power contributions to $B \to \pi, \rho$ transition form factors, Phys. Rev. D **65**, 014007 (2001).

[95] H. N. Li, Y. L. Shen, and Y. M. Wang, Next-to-leading-order corrections to $B \to \pi$ form factors in k_T factorization, Phys. Rev. D **85**, 074004 (2012).

[96] Y. Y. Keum, H. N. Li, and A. I. Sanda, Penguin enhancement and $B \to K\pi$ decays in perturbative QCD, Phys. Rev. D **63**, 054008 (2001).

[97] C. D. Lü and M. Z. Yang, B to light meson transition form-factors calculated in perturbative QCD approach, Eur. Phys. J. C **28**, 515 (2003).

[98] H. N. Li, QCD aspects of exclusive B meson decays, Prog. Part. Nucl. Phys. **51**, 85 (2003) and references therein.

[99] Z. J. Xiao, W. F. Wang, and Y. Y. Fan, Revisiting the pure annihilation decays $B_s \to \pi^+\pi^-$ and $B^0 \to K^+K^-$: The data and the perturbative QCD predictions, Phys. Rev. D **85**, 094003 (2012).

[100] Y. Y. Keum, H. N. Li, and A. I. Sanda, Fat penguins and imaginary penguins in perturbative QCD, Phys. Lett. B **504**, 6 (2001).

[101] C. D. Lü, K. Ukai, and M. Z. Yang, Branching ratio and CP violation of $B \to \pi\pi$ decays in the perturbative QCD approach, Phys. Rev. D **63**, 074009 (2001).

[102] W. Wang, Y. M. Wang, J. Xu, and S. Zhao, B-meson light-cone distribution amplitude from the Euclidean quantity, Phys. Rev. D **102**, 011502(R) (2020).

[103] M. Tanabashi *et al.* (Particle Data Group), Review of particle physics, Phys. Rev. D **98**, 030001 (2018) and 2019 update.

[104] A. V. Manohar and M. B. Wise, Heavy quark physics, Cambridge Monogr. Part. Phys., Nucl. Phys., Cosmol. **10**, 1 (2000).

[105] U. G. Meißner and W. Wang, Generalized heavy-to-light form factors in light-cone sum rules, Phys. Lett. B **730**, 336 (2014).

[106] Z. Rui, Y. Li, and H. N. Li, P-wave contributions to $B \to \psi\pi\pi$ decays in the perturbative QCD approach, Phys. Rev. D **98**, 113003 (2018).

[107] K. M. Watson, The effect of final state interactions on reaction cross sections, Phys. Rev. **88**, 1163 (1952).

[108] R. Aaij *et al.* (LHCb Collaboration), Evidence for an $\eta_c(1S)\pi^-$ resonance in $B^0 \to \eta_c(1S)K^+\pi^-$ decays, Eur. Phys. J. C **78**, 1019 (2018).

[109] R. Aaij *et al.* (LHCb Collaboration), Analysis of the resonant components in $\bar{B}^0_s \to J/\psi\pi^+\pi^-$, Phys. Rev. D **86**, 052006 (2012).

[110] C. P. Shen *et al.* (Belle Collaboration), Observation of the $\phi(1680)$ and the $Y(2175)$ in $e^+e^- \to \phi\pi^+\pi^-$, Phys. Rev. D **80**, 031101 (2009).

[111] K. Abe *et al.* (Belle Collaboration), Measurement of K^+K^- production in two photon collisions in the resonant mass region, Eur. Phys. J. C **32**, 323 (2003).

[112] S. M. Flatté, On the nature of 0^+ mesons, Phys. Lett. B **63**, 228 (1976).

[113] N. N. Achasov, V. V. Gubin, and V. I. Shevchenko, Production of scalar $K\bar{K}$ molecules in ϕ radiative decays, Phys. Rev. D **56**, 203 (1997).

[114] N. N. Achasov and A. V. Kiselev, Propagators of light scalar mesons, Phys. Rev. D **70**, 111901(R) (2004).

[115] N. N. Achasov and A. V. Kiselev, Light scalar mesons and two-kaon correlation functions, Phys. Rev. D **97**, 036015 (2018).

[116] N. N. Achasov and G. N. Shestakov, Observation of the isospin breaking decay $\Upsilon(10860) \to \Upsilon(1S)f_0(980) \to \Upsilon(1S)\eta\pi_0$ with the Belle II detector, Phys. Rev. D **96**, 091501 (2017).

[117] N. N. Achasov and V. V. Gubin, Search for the scalar a_0 and f_0 mesons in the reactions $e^+e^- \to \gamma\pi^0\pi^0(\eta)$, Phys. Rev. D **56**, 4084 (1997).

[118] N. N. Achasov and V. V. Gubin, Inadequacy of the narrow resonance approximation in $\phi \to \gamma a_0$ and $\phi \to \gamma f_0$ decays, Phys. Lett. B **363**, 106 (1995).

[119] D. V. Bugg, Reanalysis of data on $a_0(1450)$ and $a_0(980)$, Phys. Rev. D **78**, 074023 (2008).

[120] R. Aaij *et al.* (LHCb Collaboration), Measurement of resonant and CP components in $\bar{B}^0_s \to J/\psi\pi^+\pi^-$ decays, Phys. Rev. D **89**, 092006 (2014).

[121] R. Aaij *et al.* (LHCb Collaboration), Measurement of the resonant and CP components in $\bar{B}^0 \to J/\psi\pi^+\pi^-$ decays, Phys. Rev. D **90**, 012003 (2014).

[122] R. Aaij *et al.* (LHCb Collaboration), Analysis of the resonant components in $\bar{B}^0 \to J/\psi\pi^+\pi^-$, Phys. Rev. D **87**, 052001 (2013).

[123] Z. Rui, Y. Li, and Z. J. Xiao, Branching ratios, CP asymmetries and polarizations of $B \to \psi(2S)V$ decays, Eur. Phys. J. C **77**, 610 (2017).

[124] H. Y. Cheng, Y. Koike, and K. C. Yang, Two-parton light-cone distribution amplitudes of tensor mesons, Phys. Rev. D **82**, 054019 (2010).

[125] P. Colangelo, F. De Fazio, and W. Wang, $B_s \to f_0(980)$ form factors and B_s decays into $f_0(980)$, Phys. Rev. D **81**, 074001 (2010).

[126] P. Colangelo, F. De Fazio, and W. Wang, Nonleptonic B_s to charmonium decays: Analysis in pursuit of determining the weak phase β_s, Phys. Rev. D **83**, 094027 (2011).

[127] S. Cheng and J. M. Shen, $\bar{B}_s \to f_0(980)$ form factors and the width effect from light-cone sum rules, Eur. Phys. J. C **80**, 554 (2020).

[128] R. Fleischer, R. Knegjens, and G. Ricciardi, Anatomy of $B^0_{s,d} \to J/\psi f_0(980)$, Eur. Phys. J. C **71**, 1832 (2011).

[129] S. Stone and L. Zhang, Use of $B \to J/\psi f_0$ Decays to Discern the $q\bar{q}$ or Tetraquark Nature of Scalar Mesons, Phys. Rev. Lett. **111**, 062001 (2013).

[130] J. T. Daub, C. Hanhart, and B. Kubis, A model-independent analysis of final-state interactions in $\bar{B}^0_{d/s} \to J/\psi\pi\pi$, J. High Energy Phys. 02 (2016) 009.

[131] B. Aubert *et al.* (*BABAR* Collaboration), Dalitz plot analysis of the decay $B^\pm \to K^\pm K^\pm K^\mp$, Phys. Rev. D **74**, 032003 (2006).

[132] M. Ablikim *et al.* (BES Collaboration), Evidence for $f_0(980)f_0(980)$ production in χ_{c0} decays, Phys. Rev. D **70**, 092002 (2004).

[133] M. Ablikim *et al.* (BES Collaboration), Partial wave analysis of $\chi_{c0} \to \pi^+\pi^-K^+K^-$, Phys. Rev. D **72**, 092002 (2005).

[134] M. Ablikim *et al.* (BES Collaboration), Resonances in $J/\psi \to \phi\pi^+\pi^-$ and ϕK^+K^-, Phys. Lett. B **607**, 243 (2005).

[135] A. Ali, J. G. Körner, G. Kramer, and J. Willrodt, Nonleptonic weak decays of bottom mesons, Z. Phys. C **1**, 269 (1979).

[136] M. Suzuki, Final-state interactions and s-quark helicity conservation in $B \to J/\psi K^*$, Phys. Rev. D **64**, 117503 (2001).